

**Levels of symmetry adapted perturbation theory (SAPT). I. Efficiency and performance for interaction energies**

Trent M. Parker, Lori A. Burns, Robert M. Parrish, Alden G. Ryno, and C. David Sherrill

Citation: *The Journal of Chemical Physics* **140**, 094106 (2014); doi: 10.1063/1.4867135

View online: <http://dx.doi.org/10.1063/1.4867135>

View Table of Contents: <http://scitation.aip.org/content/aip/journal/jcp/140/9?ver=pdfcov>

Published by the [AIP Publishing](#)

---



## Re-register for Table of Content Alerts

Create a profile.



Sign up today!



# Levels of symmetry adapted perturbation theory (SAPT). I. Efficiency and performance for interaction energies

Trent M. Parker, Lori A. Burns, Robert M. Parrish, Alden G. Ryno, and C. David Sherrill<sup>a)</sup>

Center for Computational Molecular Science and Technology, School of Chemistry and Biochemistry,  
 and School of Computational Science and Engineering, Georgia Institute of Technology, Atlanta,  
 Georgia 30332-0400, USA

(Received 6 January 2014; accepted 17 February 2014; published online 7 March 2014)

A systematic examination of the computational expense and accuracy of Symmetry-Adapted Perturbation Theory (SAPT) for the prediction of non-covalent interaction energies is provided with respect to both method [SAPT0, DFT-SAPT, SAPT2, SAPT2+, SAPT2+(3), and SAPT2+3; with and without CCD dispersion for the last three] and basis set [Dunning cc-pVDZ through aug-cc-pV5Z wherever computationally tractable, including truncations of diffuse basis functions]. To improve accuracy for hydrogen-bonded systems, we also include two corrections based on exchange-scaling (*s*SAPT0) and the supermolecular MP2 interaction energy ( $\delta$ MP2). When considering the best error performance relative to computational effort, we recommend as the gold, silver, and bronze standard of SAPT: SAPT2+(3) $\delta$ MP2/aug-cc-pVTZ, SAPT2+/aug-cc-pVDZ, and *s*SAPT0/jun-cc-pVDZ. Their respective mean absolute errors in interaction energy across the S22, HBC6, NBC10, and HSG databases are 0.15 (62.9), 0.30 (4.4), and 0.49 kcal mol<sup>-1</sup> (0.03 h for adenine · thymine complex). © 2014 AIP Publishing LLC. [<http://dx.doi.org/10.1063/1.4867135>]

## I. INTRODUCTION

Non-covalent interactions play a central role in many applications of biological and materials chemistry.<sup>1,2</sup> A complete physical understanding of the interactions between non-bonded chemical groups is necessary to achieve the goals of optimizing drug binding or controlling the structure of organic crystals and nano self-assemblies.<sup>3</sup> The combined progress of computational hardware and software development in recent years have allowed *ab initio* quantum chemistry methods to be applied to a wide variety of complex chemical systems, including many that can provide insight into the nature of non-covalent interactions.<sup>4–7</sup>

There are two main approaches to calculating non-covalent interaction energies (IE) in quantum chemistry: supermolecular and perturbative. In the supermolecular approach, an interaction energy is the difference between the energy of the complex and the sum of the energies of each isolated monomer.<sup>8</sup> Widely used supermolecular approaches include dispersion-corrected density functional theory (DFT-D),<sup>9–11</sup> the many variants of second-order Møller–Plesset perturbation theory (MP2),<sup>12,13</sup> and coupled-cluster theory.<sup>14,15</sup> Several studies utilize coupled cluster through perturbative triples [CCSD(T)] extrapolated to the complete basis set (CBS) limit to calculate very accurate interaction energies.<sup>16</sup> Compilations of estimated CCSD(T)/CBS interaction energies (the so-called “gold-standard”<sup>17</sup> of quantum chemistry) for many bimolecular complexes constitute benchmark databases, which can be used to determine the quality of more approximate quantum chemistry methods. Widely used benchmark databases include the S22<sup>18–21</sup> and S66<sup>22,23</sup> sets of Hobza, the hydrogen-bonded curves<sup>24</sup> (HBC6) and non-

bonded curves<sup>20,25–28</sup> (NBC10) of Sherrill, and the HSG<sup>20,29</sup> set of Merz (see Sec. II C for details). Systematic studies of the accuracy of DFT and wavefunction methods relative to benchmark databases for non-covalent interactions have been carried out by Burns *et al.*<sup>30</sup> and by Hobza and co-workers.<sup>31</sup>

Perturbative approaches, by comparison, directly compute the interaction energy as a perturbation to the Hamiltonian of the individual monomers.<sup>32</sup> The most widespread of such approaches is Symmetry-Adapted Perturbation Theory<sup>33</sup> (SAPT). A key advantage over supermolecular approaches is that in addition to the interaction energy, SAPT provides a decomposition of the interaction into physical components of electrostatics, exchange, induction, and dispersion. Electrostatics includes Coulombic multipole-multipole-type interactions as well as the interpenetration of charge clouds. Exchange-repulsion is a repulsive force which arises due to monomer wavefunction overlap and the fermionic antisymmetry requirements of the dimer wavefunction. Induction includes both polarization from each monomer’s response to the other’s electric field as well as charge transfer, although the two are non-separable in SAPT. Dispersion is an attractive force resulting from the dynamical correlation between electrons on one monomer with those on another.

Recent advances in wavefunction-based SAPT theory have allowed the application of SAPT methods to chemical systems several times larger than were previously tractable. The first advance is the use of density-fitting (DF-SAPT0), which expresses a four-center two-electron integral as a product of two three-center integrals, greatly reducing the required memory and FLOPs of SAPT0 computations.<sup>34–36</sup> While previous SAPT0 implementations were only tractable with a few dozen atoms, DF-SAPT0 has been applied to systems of over 200 atoms.<sup>36</sup> The second major advance is the use of natural orbital (NO) truncations to reduce the size of the virtual space

<sup>a)</sup>Electronic mail: sherrill@gatech.edu

in high-order SAPT computations [SAPT2+, SAPT2+(3), SAPT2+3, defined in Sec. II A], resulting in a greatly reduced computational cost while incurring only miniscule errors.<sup>37,38</sup> Natural orbital truncations have allowed these computations to be performed on systems as large as adenine · thymine in an aug-cc-pVTZ basis (~1100 basis functions). These advances have recently been extended to SAPT methods employing coupled-cluster doubles (CCD) for dispersion (see Sec. II A).<sup>38</sup>

Just as with supermolecular methods like MP2 and CCSD(T), SAPT methods differ in the sophistication of their treatment of electron-electron correlation. Methods with simpler approximations for correlation (such as MP2 or SAPT0) will not be accurate at the CBS limit and thus rely on cancellation of error in small basis sets. Methods with more robust treatment of electron correlation [such as CCSD(T) or SAPT2+3] should be accurate in large basis sets and thus have larger errors in small basis sets. While wavefunction-based SAPT methods use Hartree–Fock (HF) as the reference wavefunction for monomers, it is also possible to use DFT for the monomer wavefunctions, as is done in DFT-SAPT<sup>39</sup> and SAPT(DFT).<sup>40</sup> DFT-SAPT and SAPT(DFT) compute dispersion through a time-dependent DFT (TD-DFT) response function, which provides a thorough treatment of the dispersion interaction. This more robust dispersion treatment as well as the inclusion of short-range correlation within the density functional is thought to provide accurate results without including as many terms as is required for accurate wavefunction SAPT.

Non-covalent interactions involve very subtle energy changes and electronic redistribution and thus require basis sets with both polarization and diffuse functions.<sup>16,20</sup> Correlation-consistent, augmented Dunning basis sets are an ideal choice, as they include ample polarization and diffuse functions, and they are designed to smoothly converge to the CBS limit. Due to the steep  $O(N^6)$ – $O(N^7)$  scaling of many SAPT methods (where  $N$  is proportional to system size), small decreases in the number of basis functions can result in a dramatic reduction in computational cost. Thus, we will also examine “calendar” basis sets<sup>41</sup> that systematically truncate the diffuse basis functions of the aug-cc-pVXZ Dunning basis sets ( $X = D, T, Q, \text{ or } 5$ ).

Previous studies have used a single benchmark database and/or anecdotal cases to examine the accuracy of a few SAPT methods with one or a few basis sets.<sup>16,42</sup> In this work we aim to provide a systematic examination of the accuracy of SAPT methods for predicting non-covalent interaction energies across a widely representative subset of chemical interaction space. We aim to find those model chemistries (method + basis set) that provide the greatest accuracy relative to computational effort, so called “Pauling points.”<sup>43,44</sup> We also seek to identify any general weaknesses in this set of SAPT methods and introduce corrections to improve performance without increasing computational cost.

## II. THEORETICAL METHODS

### A. SAPT methods

The SAPT interaction energy can be written as a perturbation series:<sup>33</sup>

$$E_{\text{IE}}^{\text{SAPT}} = \sum_{n=1}^{\infty} \sum_{k=0}^{\infty} \sum_{l=0}^{\infty} (E_{\text{pol}}^{(nkl)} + E_{\text{exch}}^{(nkl)}), \quad (1)$$

where (usually) attractive terms originating from the *polarization expansion* and repulsive terms originating from antisymmetry arguments are expanded in orders of the intermolecular potential,  $n$ , and intramonomer electron correlation,  $k$  and  $l$ . The SAPT series can be truncated according to desired accuracy and the size and nature of the molecular system under consideration. Several established levels are defined below (and compared visually in Fig. 1), with terms labeled such that  $E^{(vw)}$  reflects the order in  $v = n$  and  $w = k + l$ . This definition naturally leads to terms which can be interpreted as belonging to one of four physically motivated components: electrostatics, exchange, induction, and dispersion. Eqs. (2)–(16) indicate within brackets the physical component to which each computed term belongs according to our partitioning scheme. The detailed definitions of the particular terms  $E^{(vw)}$  in the equations below may be found in Refs. 45–47.

The simplest SAPT method, SAPT0, essentially treats the monomers at the Hartree–Fock level and appends explicit dispersion terms emerging from second-order perturbation theory to the electrostatics, exchange, and induction terms inherited from a HF dimer treatment. With the imposition of density fitting,<sup>34</sup> SAPT0 is inexpensive and comparable in cost to a DF-MP2 calculation. The SAPT0 IE is defined by

$$\begin{aligned} E_{\text{IE}}^{\text{SAPT0}} &= E_{\text{IE}}^{\text{HF}} + [E_{\text{disp}}^{(20)} + E_{\text{exch-disp}}^{(20)}]_{\text{disp}} \\ &= [E_{\text{elst}}^{(10)}]_{\text{elst}} + [E_{\text{exch}}^{(10)}]_{\text{exch}} \\ &\quad + [E_{\text{ind,r}}^{(20)} + E_{\text{exch-ind,r}}^{(20)} + \delta E_{\text{HF}}^{(2)}]_{\text{ind}} + [E_{\text{disp}}^{(20)} + E_{\text{exch-disp}}^{(20)}]_{\text{disp}}. \end{aligned} \quad (2)$$

The Hartree–Fock correction,  $\delta E_{\text{HF}}^{(2)}$ , is defined in Eq. (4) so as to satisfy the equality between Eqs. (2) and (3). This term primarily represents polarization beyond the second-order  $E_{\text{ind}}^{(20)}$ .

$$\begin{aligned} \delta E_{\text{HF}}^{(2)} &\equiv E_{\text{IE}}^{\text{HF}} - ([E_{\text{elst}}^{(10)}]_{\text{elst}} + [E_{\text{exch}}^{(10)}]_{\text{exch}} \\ &\quad + [E_{\text{ind,r}}^{(20)} + E_{\text{exch-ind,r}}^{(20)}]_{\text{ind}}). \end{aligned} \quad (4)$$

Spin-component scaling (SCS) has been applied to MP2 and CCSD as a way of improving performance for non-covalent interactions and other applications.<sup>12,48</sup> Here we analogously define SCS-SAPT0, which uses same-spin (SS) and opposite-spin (OS) parameters to scale the dispersion and exchange-dispersion terms, leaving electrostatics, exchange, and induction components unchanged from SAPT0. Data presented here use values of  $p_{\text{SS}} = 2/3$  and  $p_{\text{OS}} = 6/5$ , which are optimal over all four test sets when using the jun-cc-pVDZ basis set which is best for SAPT0. No other choice of  $p_{\text{SS}}$  or  $p_{\text{OS}}$  significantly improves the performance of SCS-SAPT0,

$$\begin{aligned} E_{\text{IE}}^{\text{SCS-SAPT0}} &= E_{\text{IE}}^{\text{HF}} + [p_{\text{SS}}(E_{\text{SS-disp}}^{(20)} + E_{\text{SS-exch-disp}}^{(20)}) \\ &\quad + p_{\text{OS}}(E_{\text{OS-disp}}^{(20)} + E_{\text{OS-exch-disp}}^{(20)})]_{\text{disp}}. \end{aligned} \quad (5)$$

Another variant newly defined here, sSAPT0, involves minor tweaks to the SAPT0  $E_{\text{exch-ind}}^{(20)}$  and  $E_{\text{exch-disp}}^{(20)}$  values.

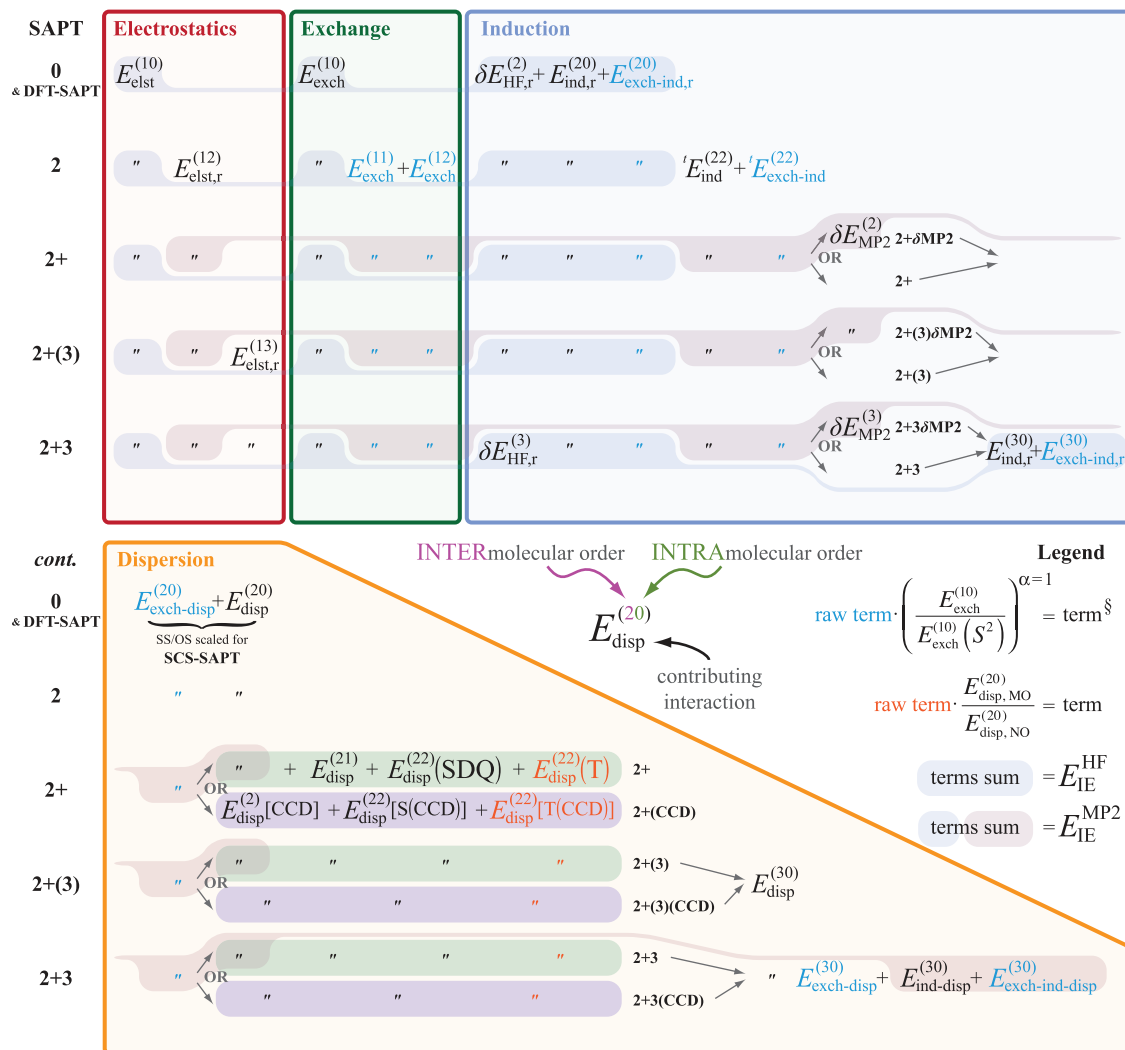


FIG. 1. Composition of all 17 SAPT methods examined. The additive nature of terms that define SAPT methods is shown, along with their apportionment into physical components. SAPT2+, SAPT2+(3), and SAPT2+3 can include  $\delta\text{MP2}$  correction (upper path at Induction bifurcation) or omit it (lower path) and include MP4 (upper path at Dispersion bifurcation) or CCD (lower path) dispersion.  $\S$ See Ref. 50 for details regarding turquoise-blue exchange terms.

While  $E_{\text{exch}}^{(10)}$  is calculated using an analytic formula,  $E_{\text{exch-ind}}^{(20)}$  and  $E_{\text{exch-disp}}^{(20)}$  utilize an approximation based on the second power of the orbital overlap ( $S^2$ ), which breaks down at short intermolecular distances. Lao and Herbert noticed a similar breakdown in third-order exchange-induction,  $E_{\text{exch-ind}}^{(30)}$ , and applied a similar correction to that which we describe below.<sup>49</sup> The ratio of the analytically computed  $E_{\text{exch}}^{(10)}$  to the approximation  $E_{\text{exch}}^{(10)}(S^2)$  gives a scale factor  $p_{\text{EX}}$ , which can be further modulated by an exponent,  $\alpha$ ,

$$p_{\text{EX}}(\alpha) = \left( \frac{E_{\text{exch}}^{(10)}}{E_{\text{exch}}^{(10)}(S^2)} \right)^{\alpha}. \quad (6)$$

In this work, all exchange-type terms in wavefunction SAPT are scaled by this factor with  $\alpha = 1.0$  unless otherwise noted; this choice assumes that the breakdown in the  $S^2$  approximation occurs in a similar manner for all exchange-like terms as it does for  $E_{\text{exch}}^{(10)}$ . We will be recommending the choice of  $\alpha = 1.0$  for future work in wavefunction-based SAPT, as noted in Ref. 50, and as was done previously in Ref. 51. In many cases,  $\delta E_{\text{HF}}$  or  $\delta E_{\text{MP2}}$  cancels out this correction such

that only the components and not the IE are affected. See Ref. 50 for more details on exchange-scaling. For  $s\text{SAPT0}$  only, we choose  $\alpha = 3.0$  on the basis of results for the HBC6 test set (which focuses on H-bonding, where the exchange scaling has the largest effect), and the value of  $\delta E_{\text{HF}}$  is left unchanged from Eq. (4) computed with  $p_{\text{EX}}(1.0)$ . The resulting  $s\text{SAPT0}$  energy expression is

$$E_{\text{IE}}^{s\text{SAPT0}} = [E_{\text{elst}}^{(10)}]_{\text{elst}} + [E_{\text{exch}}^{(10)}]_{\text{exch}} + [E_{\text{ind},r}^{(20)} + p_{\text{EX}}(3.0)E_{\text{exch-ind},r}^{(20)} + \delta E_{\text{HF}}^{(2)}]_{\text{ind}} + [E_{\text{disp}}^{(20)} + p_{\text{EX}}(3.0)E_{\text{exch-disp}}^{(20)}]_{\text{disp}}. \quad (7)$$

The result is an IE which is always more positive (less bound). This corrects for very strong overbinding of SAPT0 at short range, especially for strongly interacting systems such as double hydrogen bonds. The choice of  $\alpha = 3.0$  is empirical and results in the minimum errors for HB systems in the jun-cc-pVDZ basis set (see Sec. II B) with respect to the value of  $\alpha$ .



While employing the same SAPT0 treatment for dispersion, SAPT2 adds terms for electrostatics, exchange, and induction up to second-order with respect to intramonomer electron correlation. This is one of the most commonly applied levels due to its availability in the SAPT software by Szalewicz and co-workers,<sup>52</sup> and it performs similarly to MP2, hence its suitability only for electrostatics-, not dispersion-dominated, systems,

$$E_{\text{IE}}^{\text{SAPT2}} = E_{\text{IE}}^{\text{SAPT0}} + [E_{\text{elst},r}^{(12)}]_{\text{elst}} + [E_{\text{exch}}^{(11)} + E_{\text{exch}}^{(12)}]_{\text{exch}} + [{}^t E_{\text{ind}}^{(22)} + {}^t E_{\text{exch-ind}}^{(22)}]_{\text{ind}}. \quad (8)$$

In SAPT2+ and beyond, intramonomer corrections to dispersion are summed through second-order at a level similar to MP4 and thus incurs a steep  $O(N^7)$  scaling. As SAPT2+ and SAPT2+(3) differ only by two  $O(N^6)$  terms, the latter, more complete, method would seem to be preferable. The heavy cost of the perturbative triples term may be substantially ameliorated by expressing it in terms of MP2 natural orbitals then truncating the virtual orbital space by half or more with minimal loss of accuracy. The procedure employed here involves both a natural orbital truncation ( $10^{-6}$  electrons occupation cutoff) and concomitant scaling of the  $E_{\text{disp}}^{(22)}(T)$  term as described in Ref. 16. SAPT2+3 extends SAPT2+(3) with third-order induction terms as well as the coupling between induction and dispersion, making it more computationally expensive by a small fraction,

$$E_{\text{IE}}^{\text{SAPT2+}} = E_{\text{IE}}^{\text{SAPT2}} + [E_{\text{disp}}^{(21)} + E_{\text{disp}}^{(22)}]_{\text{disp}}, \quad (9)$$

$$E_{\text{IE}}^{\text{SAPT2+(3)}} = E_{\text{IE}}^{\text{SAPT2+}} + [E_{\text{elst},r}^{(13)}]_{\text{elst}} + [E_{\text{disp}}^{(30)}]_{\text{disp}}, \quad (10)$$

$$E_{\text{IE}}^{\text{SAPT2+3}} = E_{\text{IE}}^{\text{SAPT2+(3)}} + [E_{\text{ind},r}^{(30)} + E_{\text{exch-ind},r}^{(30)}]_{\text{ind}} + [E_{\text{exch-disp}}^{(30)} + E_{\text{ind-disp}}^{(30)} + E_{\text{exch-ind-disp}}^{(30)}]_{\text{disp}}. \quad (11)$$

The third-order induction terms in SAPT2+3 are included in an updated, third-order  $\delta E_{\text{HF}}^{(3)}$ :

$$\delta E_{\text{HF}}^{(3)} \equiv E_{\text{IE}}^{\text{HF}} - ([E_{\text{elst}}^{(10)}]_{\text{elst}} + [E_{\text{exch}}^{(10)}]_{\text{exch}} + [E_{\text{ind},r}^{(20)} + E_{\text{exch-ind},r}^{(20)} + E_{\text{ind},r}^{(30)} + E_{\text{exch-ind},r}^{(30)}]_{\text{ind}}). \quad (12)$$

Hence, when  $\delta E_{\text{HF}}^{(3)}$  is included, the additional terms  $E_{\text{ind},r}^{(30)}$  and  $E_{\text{exch-ind},r}^{(30)}$  do not contribute directly to the overall interaction energy because they are cancelled by  $\delta E_{\text{HF}}^{(3)}$ . For non-polar molecules, results can be more accurate if this term is omitted.<sup>53</sup> Here we include  $\delta E_{\text{HF}}^{(3)}$  in all SAPT2+3 results to simplify the analysis.

While these high-order SAPT methods are found to reliably describe all but the most difficult dispersion-bound systems, electrostatically dominated complexes are often helped by the addition of a MP2 correction. Just as  $\delta E_{\text{HF}}$  accounts for missing higher-order polarization in the perturbation series truncation,  $\delta E_{\text{MP2}}$  accounts for missing terms such as high-order coupling between induction and dispersion. This term cannot be rigorously classified as either induction or dispersion, and we make the arbitrary decision to group it within induction. In most cases  $\delta E_{\text{MP2}}$  is quite small, and the effect on the SAPT component values is minimal. Cases where  $\delta E_{\text{MP2}}$

becomes large are those where the second- or third-order truncation of the SAPT perturbation series begins to fail, and the meaning of the components begins to break down.

We define  $\delta E_{\text{MP2}}$  by the difference between the SAPT2 and MP2 interaction energies:

$$\delta E_{\text{MP2}} \equiv E_{\text{IE}}^{\text{MP2}} - E_{\text{IE}}^{\text{SAPT2}}. \quad (13)$$

For SAPT2+, SAPT2+(3), and SAPT2+3, the analogous MP2-corrected method is created by adding  $\delta E_{\text{MP2}}$  to each method to produce SAPT2+ $\delta$ MP2, SAPT2+(3) $\delta$ MP2, and SAPT2+3 $\delta$ MP2, respectively. This is equivalent to replacing  $E_{\text{IE}}^{\text{SAPT2}}$  in Eqs. (9)–(11) with  $E_{\text{IE}}^{\text{MP2}}$  such that

$$E_{\text{IE}}^{\text{SAPT2+}\delta\text{MP2}} = E_{\text{IE}}^{\text{SAPT2+}} + [\delta E_{\text{MP2}}]_{\text{ind}}, \quad (14)$$

$$E_{\text{IE}}^{\text{SAPT2+(3)}\delta\text{MP2}} = E_{\text{IE}}^{\text{SAPT2+(3)}} + [\delta E_{\text{MP2}}]_{\text{ind}}, \quad (15)$$

$$E_{\text{IE}}^{\text{SAPT2+3}\delta\text{MP2}} = E_{\text{IE}}^{\text{SAPT2+3}} + [\delta E_{\text{MP2}}]_{\text{ind}}. \quad (16)$$

Here,  $E_{\text{IE}}^{\text{MP2}}$  are always counterpoise (CP) corrected using the scheme of Boys and Bernardi<sup>54</sup> and utilize density fitting (DF-MP2). Density fitting in DF-MP2 incurs errors in IE which are smaller than the decimal place reported here (hundredths of a kcal mol<sup>-1</sup>).

For the three high-order wavefunction-based SAPT methods, one has a choice to use MP4-level dispersion terms or to compute dispersion with  $t_2$  amplitudes from CCD,<sup>46</sup> giving rise to six SAPT(CCD) variants (the three levels with and without  $\delta$ MP2). This affects only the dispersion term, leaving electrostatics, exchange, and induction unaltered. The CCD dispersion in principle should be a more robust treatment of dispersion. We can compare and contrast the dispersion in SAPT2+ and SAPT2+(CCD):

$$E_{\text{disp}}^{\text{SAPT2+}} = E_{\text{exch-disp}}^{(20)} + E_{\text{disp}}^{(20)} + E_{\text{disp}}^{(21)} + E_{\text{disp}}^{(22)}(\text{SDQ}) + E_{\text{disp}}^{(22)}(T), \quad (17)$$

$$E_{\text{disp}}^{\text{SAPT2+(CCD)}} = E_{\text{exch-disp}}^{(20)} + E_{\text{disp}}^{(2)}[\text{CCD}] + E_{\text{disp}}^{(22)}[\text{S(CCD)}] + E_{\text{disp}}^{(22)}[\text{T(CCD)}]. \quad (18)$$

Then we can similarly define the dispersion term for SAPT2+(3)(CCD) and SAPT2+3(CCD) by adding the necessary additional terms from SAPT2+(3) and SAPT2+3:

$$E_{\text{disp}}^{\text{SAPT2+(3)}(\text{CCD})} = E_{\text{disp}}^{\text{SAPT2+(CCD)}} + E_{\text{disp}}^{(30)}, \quad (19)$$

$$E_{\text{disp}}^{\text{SAPT2+3}(\text{CCD})} = E_{\text{disp}}^{\text{SAPT2+(3)}(\text{CCD})} + E_{\text{exch-disp}}^{(30)} + E_{\text{ind-disp}}^{(30)} + E_{\text{exch-ind-disp}}^{(30)}. \quad (20)$$

In addition to wavefunction SAPT methods, which use a HF reference wavefunction, density functional based approaches have been developed in two flavors: DFT-SAPT<sup>55,56</sup> by Heßelmann and co-workers and SAPT(DFT)<sup>39,40,57,58</sup> by Szalewicz and co-workers. These methods include analogous terms to SAPT0 (see Eq. (3)), scale as  $O(N^5)$ , and have been shown to be reliable, especially for challenging dispersion problems.<sup>51,59</sup> This work uses DFT-SAPT as encoded in MOLPRO which employs density-fitting extensively. The formulation is LPBE0AC, defined in Ref. 56, that computes the

SAPT portion with ALDA and the monomers with PBE0 using local Hartree–Fock exchange. Monomers also incorporate an asymptotic correction by LB94 based upon the difference between the PBE0 HOMO energy and its vertical ionization potential. This parameter was computed for each monomer with an augmented quadruple- $\zeta$  basis set and subsequently employed for DFT-SAPT computations with all basis sets. The DFT-SAPT interaction energies reported include a  $\delta$ HF correction computed identically to that in wavefunction-based SAPT0. In a few cases when SAPT terms were so close to zero that the code was unable to properly compute the value, typically at the tails of dissociation curves in smaller basis sets, terms were manually set to zero through the MOLPRO SAPT driver.

## B. Basis sets

SAPT methods were evaluated with the double-, triple-, quadruple-, and quintuple- $\zeta$  ( $X\zeta$ , for  $X = D, T, Q$ , and  $5$ , respectively) basis sets of Dunning augmented by diffuse functions on all atoms.<sup>60,61</sup> These are denoted as aug-cc-pVDZ (aDZ), aug-cc-pVTZ (aTZ), aug-cc-pVQZ (aQZ), and aug-cc-pV5Z (a5Z) throughout. Truncations of the diffuse space have long been used, notably heavy-aug-cc-pVXZ (haXZ, which places cc-pVXZ on hydrogen or helium and aug-cc-pVXZ on all heavier atoms) and aug-cc-pVDZ' which has been recommended<sup>36</sup> for SAPT0. Papajak and Truhlar have systematized such truncations by defining a new basis set for each diffuse shell removed and naming it after a calendar month (counting back from August or fully augmented).<sup>62</sup> These are referred to as *calendar* basis sets and their construction is detailed in Table I. The aug-cc-pVDZ' set mentioned previously is identical to jun-cc-pVDZ (jaDZ). Generally, all D $\zeta$ , T $\zeta$ , and Q $\zeta$  calendar basis sets and a5Z were considered for SAPT0 and all D $\zeta$ , T $\zeta$ , and aQZ for DFT-SAPT, while SAPT2 and higher perturbation levels were confined to D $\zeta$  and T $\zeta$ .

Efficient implementations of SAPT methods employ density-fitting and thus require specification of auxiliary basis sets, and calendar basis sets present additional choices. For the most part, the defaults for Dunning basis sets suggested by MOLPRO and PSI4 were employed. In keeping with MOLPRO DFT-SAPT defaults, fully augmented aXZ orbital basis sets employ aug-cc-pVXZ-JKFIT, aug-cc-pVXZ-RI, and cc-pVXZ-JKFIT for density-fitting roles in IE Coulomb/exchange and monomer local HF, MP2 dis-

persion, and monomer Coulomb/exchange, respectively. The un-augmented XZ orbital bases analogously use cc-pVXZ-JKFIT, cc-pVXZ-RI, and cc-pVXZ-JKFIT. For the intervening calendar orbital basis sets, haXZ, jaXZ, maXZ, and aaXZ, MOLPRO computations in this work use the same auxiliary sets as the corresponding aXZ basis. In contrast, PSI4 has built into it -JKFIT and -RI basis sets that are truncated analogously to the construction of the calendar orbital bases. The wavefunction SAPT computations thus use, for example, may-cc-pVTZ-JKFIT and may-cc-pVTZ-RI as auxiliaries to the may-cc-pVTZ orbital basis set.

## C. Gold standard databases

Databases S22, NBC10, HBC6, and HSG provide high quality reference values and have been employed here for benchmarking SAPT interaction energies. These databases are composed of binary complexes and (i) strive to be typical of “real-world” nonbonding interactions, (ii) encompass a variety of structural arrangements and intermonomer distances, and (iii) support high-level interaction energy benchmarks. Reference values typically are obtained through estimation of the CBS limit through a 2-stage basis set refinement procedure where a coupled-cluster correction,  $\delta_{\text{MP2}}^{\text{CCSD(T)}}$ , of at least T $\zeta$  quality is appended to a MP2 interaction energy of at least extrapolated T $\zeta$ –Q $\zeta$  quality. This work uses the recently revised benchmarks of Ref. 20 for all databases (Revision B for S22, Revision A for others). Consult the supplementary material for a tabulation of the exact CBS treatment for each database member.<sup>63</sup> Summary IE quantities for each benchmark set are available in Table II.<sup>64,65</sup>

S22. Jurečka and co-workers designed a compact database representative of nonbonded interactions varying in size from very small (e.g., water dimer) to substantial (e.g., adenine·thymine complex), denoted S22.<sup>18</sup> The set is constructed from balanced contributions by 7 hydrogen-bonded (HB), 8 mixed influence (MX), and 7 dispersion bound (DD) complexes (after the SAPT2+(3)-guided reapportionment described in Ref. 20).

NBC10. Dissociation curves for ten molecular systems with frozen-structure monomers at 184 geometries form a database named *Non-Bonded Curves* or NBC10. Members include the sandwich (DD), T-shaped (DD), and 3.2 (MX), 3.4 (DD), and 3.6 (DD) Å-separated parallel-displaced configurations of the benzene dimer, benzene·hydrogen sulfide (MX), benzene·methane (DD), methane dimer (DD), the

TABLE I. Levels of truncation for diffuse functions in standard basis sets.

Augmentation level	Angular momenta in the diffuse space <sup>a</sup>		Valid basis sets		
	Li–Kr main group	H & He	D $\zeta$	T $\zeta$	Q $\zeta$
aug-cc-pVXZ	s, p, ..., $\ell_{\text{max}} - 2$ , $\ell_{\text{max}} - 1$ , $\ell_{\text{max}}$	s, p, ..., $\ell_{\text{max}} - 1$	aDZ	aTZ	aQZ
heavy-aug- OR jul-cc-pVXZ	s, p, ..., $\ell_{\text{max}} - 2$ , $\ell_{\text{max}} - 1$ , $\ell_{\text{max}}$		haDZ	haTZ	haQZ
jun-cc-pVXZ	s, p, ..., $\ell_{\text{max}} - 2$ , $\ell_{\text{max}} - 1$		jaDZ	jaTZ	jaQZ
may-cc-pVXZ	s, p, ..., $\ell_{\text{max}} - 2$			maTZ	maQZ
...	s, p				aaQZ
cc-pVXZ			DZ	TZ	QZ

<sup>a</sup>  $\ell_{\text{max}} = 2$  or d for D $\zeta$ ;  $\ell_{\text{max}} = 3$  or f for T $\zeta$ ;  $\ell_{\text{max}} = 4$  or g for Q $\zeta$ .

TABLE II. Database statistics. Interaction energy (kcal/mol) means and ranges (in parentheses) are presented for each database and subcategory.

Database	Hydrogen bonded		Mixed influence		Dispersion bound		Overall	
S22	−13.88	(−20.64, −3.13)	−5.74	(−11.73, −1.50)	−2.51	(−4.52, −0.53)	−7.30	(−20.64, −0.53)
NBC10/HBC6	−10.69	(−26.06, −0.13)	−1.14	(−2.95, +9.34)	−1.30	(−2.89, +3.46)	−4.94 <sup>a</sup>	(−26.06, +9.34)
NBC10/HBC6 <sup>b</sup>	−18.05	(−26.06, −15.65)	−2.52	(−2.95, −1.89)	−2.04	(−2.89, −0.42)	−7.88 <sup>a</sup>	(−26.06, −0.42)
HSG	−15.05	(−19.08, −9.54)	−6.21	(−7.51, −5.07)	−1.25	(−3.31, +0.38)	−4.17	(−19.08, +0.38)

<sup>a</sup>Average performed over both HBC and NBC test sets.<sup>b</sup>For each dissociation curve, includes only five points contiguous to minimum.

anti-parallel sandwich (DD) pyridine dimer, and a T-shaped (MX) pyridine dimer. Bonding motifs (in parentheses) have been reassigned on the basis of SAPT2+(3) decompositions.

**HBC6.** A database of fully relaxed dissociation curves for six molecular systems comprising 118 geometries is denoted *Hydrogen-Bonded Curves* or *HBC6*.<sup>24</sup> The set is composed of formic acid, formamide, and formamidine monomers in three homogeneous and three mixed complexes. Together, these encompass many of the most common hydrogen bonding patterns, including O...H...O, O...H...N, and N...H...N.

**HSG.** Merz and co-workers examined an HIV-II protease protein with a bound indinavir ligand and decomposed the docking site into 21 pairs of chemical fragments designated *HSG*.<sup>29</sup> The resulting complexes contain between 19 and 32 atoms and are particularly challenging for quantum chemical methods since geometries are not necessarily equilibrium configurations. Since the publication of Ref. 20, a few members have been reallocated (guided strictly by SAPT decomposition) among the customary HB, MX, and DD subsets.

## D. Technical details

Wavefunction SAPT methods have been accessed through BETA3 and later releases of the quantum chemistry code PSI4.<sup>66</sup> DFT-SAPT computations and MP2 interaction energies for  $\delta$ MP2 were performed with MOLPRO<sup>67</sup> 2009.1 and 2010.1. Timing results were generated on hardware featuring Xeon Core i7-3930K processors (6 cores, overclocked to 3.9 GHz) and 64 GB memory. Computations were run fully threaded across six processors through Intel MKL 10.3. The system used for comparing timings is S22-7, a Watson–Crick-bonded adenine·thymine complex of  $C_1$  symmetry.

The performance of a method and basis set (together, a theoretical model chemistry<sup>68</sup>) for a given test set is evaluated by comparing the interaction energy (always in kcal mol<sup>−1</sup>) for each individual system to that of its reference interaction energy value [est. CCSD(T)/CBS] and is summarized by the quantity mean absolute error (MAE =  $\frac{1}{n} \sum_{sys}^n |\text{SAPT}_{sys} - \text{REF}_{sys}|$ ). Other error metrics such as mean absolute percent error (MA%E), minimum and maximum error, root-mean-square error (RMSE), and mean signed error (MSE) have advantages and disadvantages as discussed fully in Sec. II C of Ref. 30. These metrics are also defined and presented for all model chemistries in the supplementary material<sup>63</sup> analogously to Tables III–V of this article. Where applicable, statistics for subgroups [i.e., Hydrogen Bonded (HB), Mixed Influence (MX), Dispersion Bound

(DD)] of test sets are collected. It is readily gleaned that underbinding errors are positive and overbound are negative.

## E. Reading strip charts

While summary statistics are valuable, a model chemistry can be more completely assessed by a visual representation of errors from all database members. Results for several of the best methods examined in this work are illustrated by strip charts included in Tables III–V, the conventions for which are outlined here. Each horizontal strip represents the results for the four databases (S22, NBC10, HBC6, and HSG) with a given model chemistry. Thin vertical lines plot the error in interaction energy (kcal mol<sup>−1</sup>) for each member of the test set in either the underbound (right of the zero-error line) or overbound (left of the zero-error line) sector of the chart. Individual quantities lying beyond the range of the graph are omitted without annotation. The vertical lines are colored to indicate the member belongs to the hydrogen-bonded (red), mixed-influence (green), or dispersion-bound (blue) subsets. A black rectangular marker indicates the MAE over all the databases, with its position being fixed in the “overbound” sector of the graph for ease of comparison to the zero line, regardless of the preponderance of individual subset markings. For databases composed of potential energy curves (i.e., NBC10 and HBC6), only five points centered on the equilibrium geometry of each curve are plotted and used to compute the MAE marker position; this strategy avoids the visual confusion that would arise from the many small-error points at the tail of a curve that are not directly comparable to the minimum-energy values in other test sets.



## III. RESULTS AND DISCUSSION

The most condensed summaries of examined SAPT model chemistries are presented through MAE statistics by database and binding motif in Table III for double- $\zeta$  basis sets, Table IV for triple- $\zeta$  basis sets, and Table V for aQZ and a5Z basis sets. More detailed summaries including all methods and basis sets are presented in the supplementary material,<sup>63</sup> along with all individual database member interaction energy values at each model chemistry and individual reference values. Graphical comparisons of model chemistries by performance and efficiency are given in Figs. 2 and 3, respectively.

### A. SAPT0

The simplest SAPT method, SAPT0, through favorable cancellation of errors, performs best with the truncated

TABLE III. Mean absolute error (kcal mol<sup>-1</sup>) of the interaction energy for databases and their subsets with double- $\zeta$  basis sets. Full tables for all SAPT methods and basis sets located in the supplementary material.<sup>63</sup>

Method & Basis Set	S22			Overall			Error Distribution <sup>a</sup>							Time <sup>b</sup>	
	HB	MX/DD	TT	HB	MX/DD	TT	4	OB	1	0	1	UB	4		
aug-cc-pVDZ															
DFT-SAPT	1.92	0.59	1.01	2.00	0.37	0.99								4.6 <sup>b</sup>	
SAPT0	2.02	1.17	1.44	2.45	0.86	1.73								0.1	
sSAPT0	1.70	1.15	1.32	1.82	0.84	1.35								0.1	
SCS-SAPT0	1.72	0.79	1.09	2.10	0.60	1.44								0.1	
SAPT2	1.44	0.70	0.94	1.33	0.61	0.89								0.4	
SAPT2+	0.45	0.26	0.32	0.46	0.17	0.30								SILVER 	4.4
SAPT2+(3)	0.71	0.26	0.40	0.67	0.21	0.39								4.7	
SAPT2+3	0.38	0.24	0.29	0.50	0.14	0.28								5.2	
SAPT2+3 $\delta$ MP2	0.85	0.25	0.44	1.10	0.20	0.65								5.2	
SAPT2+3(CCD)	0.60	0.33	0.42	0.65	0.27	0.40								10.2	
SAPT2+3(CCD) $\delta$ MP2	1.07	0.57	0.73	1.35	0.43	0.89								10.2	
heavy-aug-cc-pVDZ															
DFT-SAPT	2.14	0.72	1.17	2.28	0.52	1.19								3.7 <sup>b</sup>	
SAPT0	1.92	1.12	1.38	2.27	0.80	1.64								0.1	
sSAPT0	1.59	1.10	1.26	1.63	0.78	1.25								0.1	
SCS-SAPT0	1.62	0.75	1.03	1.92	0.56	1.36								0.1	
SAPT2	1.55	0.69	0.96	1.47	0.61	0.93								0.3	
SAPT2+	0.64	0.29	0.40	0.59	0.23	0.37								3.3	
SAPT2+(3)	0.90	0.35	0.52	0.90	0.31	0.52								3.5	
SAPT2+3	0.57	0.31	0.39	0.69	0.22	0.39								3.7	
SAPT2+3 $\delta$ MP2	1.05	0.35	0.57	1.36	0.33	0.82								3.7	
SAPT2+3(CCD)	0.80	0.47	0.57	0.87	0.40	0.56								7.9	
SAPT2+3(CCD) $\delta$ MP2	1.28	0.70	0.88	1.62	0.58	1.08								7.9	
jun-cc-pVDZ															
DFT-SAPT	3.30	1.59	2.13	3.68	1.22	2.20								3.4 <sup>b</sup>	
SAPT0	0.80	0.32	0.47	1.26	0.32	0.86								0.0	
sSAPT0	0.49	0.30	0.36	0.71	0.31	0.49								BRONZE 	0.0
SCS-SAPT0	0.55	0.44	0.47	1.07	0.45	0.85								0.0	
SAPT2	2.65	0.74	1.34	2.70	0.64	1.41								0.2	
SAPT2+	1.84	1.10	1.34	1.80	0.92	1.24								1.6	
SAPT2+(3)	2.07	1.32	1.56	2.18	1.06	1.47								1.7	
SAPT2+3	1.75	1.13	1.33	1.88	0.94	1.25								1.8	
SAPT2+3 $\delta$ MP2	2.41	1.40	1.72	2.94	1.14	1.95								1.8	
SAPT2+3(CCD)	1.96	1.46	1.62	2.09	1.16	1.47								3.8	
SAPT2+3(CCD) $\delta$ MP2	2.62	1.73	2.02	3.17	1.36	2.19								3.8	

<sup>a</sup>Errors with respect to Gold Standard (see Sec. II E for plot details). Guide lines are at 0, 0.3, and 1.0 kcal/mol overbound (−) and underbound (+).

<sup>b</sup>Time (hours) to compute adenine · thymine complex. See also Ref. 70.

double- $\zeta$  basis set jun-cc-pVDZ. SAPT0/jaDZ has a MAE of 0.32 kcal mol<sup>-1</sup> for MX and DD complexes and 1.26 kcal mol<sup>-1</sup> for HB systems across all four benchmark databases. This semi-quantitative accuracy is acceptable for most applications which aim to gain the insight of the SAPT physical decomposition without need for the highest levels of accuracy. Errors for all binding motif subsets increase with

any basis set larger than jaDZ as seen in Fig. 2(a). The cc-pVDZ basis is too small due to the lack of diffuse functions and has larger errors than jaDZ as well.

SAPT0/jaDZ performs better for highly polarizable DD complexes such as the benzene dimer than less polarizable complexes such as the methane dimer. This trend is explained by the similarity of SAPT0 and MP2. For highly polarizable



TABLE IV. Mean absolute error (kcal mol<sup>-1</sup>) of the interaction energy for databases and their subsets with triple- $\zeta$  basis sets. Full tables for all SAPT methods and basis sets located in the supplementary material.<sup>63</sup>

Method & Basis Set	S22			Overall			Error Distribution <sup>a</sup>							Time <sup>b</sup>
	HB	MX/DD	TT	HB	MX/DD	TT	4	OB	1	0	1	UB	4	
aug-cc-pVTZ														
DFT-SAPT	1.01	0.21	0.47	0.92	0.14	0.38								16.8 <sup>b</sup>
SAPT0	2.75	1.53	1.92	3.40	1.12	2.33								0.5
SAPT2	0.32	1.07	0.84	0.55	0.84	0.82								4.9
SAPT2+	0.77	0.63	0.67	1.37	0.46	0.95								55.8
SAPT2+(3)	0.46	0.25	0.32	0.79	0.18	0.54								62.9
SAPT2+3	0.83	0.54	0.63	1.24	0.35	0.88								74.9
SAPT2+ $\delta$ MP2	0.34	0.48	0.44	0.47	0.31	0.36								55.8
SAPT2+(3) $\delta$ MP2	0.16	0.16	0.16	0.24	0.13	0.15								62.9
SAPT2+3 $\delta$ MP2	0.16	0.22	0.21	0.21	0.14	0.14								74.9
SAPT2+(CCD)	0.51	0.23	0.32	1.08	0.19	0.67								114.9
SAPT2+(3)(CCD)	0.23	0.20	0.21	0.51	0.19	0.43								122.1
SAPT2+3(CCD)	0.59	0.20	0.32	0.95	0.16	0.66								134.1
SAPT2+(CCD) $\delta$ MP2 <sup>c</sup>	0.13	0.10	0.11	0.22	0.09	0.12								114.9
SAPT2+(3)(CCD) $\delta$ MP2	0.32	0.30	0.31	0.43	0.26	0.35								122.1
SAPT2+3(CCD) $\delta$ MP2	0.23	0.19	0.21	0.31	0.18	0.23								134.1
jun-cc-pVTZ														
DFT-SAPT	1.36	0.44	0.73	1.30	0.27	0.61								11.3 <sup>b</sup>
SAPT0	2.46	1.31	1.68	3.05	0.94	2.09								0.2
SAPT2	0.54	0.89	0.78	0.65	0.72	0.74								2.1
SAPT2+	0.43	0.37	0.39	0.95	0.23	0.65								27.1
SAPT2+(3)	0.24	0.19	0.21	0.50	0.16	0.40								29.9
SAPT2+3	0.58	0.32	0.40	0.88	0.16	0.62								33.5
SAPT2+ $\delta$ MP2	0.20	0.27	0.25	0.20	0.16	0.17								27.1
SAPT2+(3) $\delta$ MP2	0.40	0.21	0.27	0.55	0.21	0.37								29.9
SAPT2+3 $\delta$ MP2	0.33	0.17	0.22	0.43	0.16	0.28								33.5
SAPT2+(CCD)	0.24	0.11	0.15	0.70	0.12	0.45								58.0
SAPT2+(3)(CCD)	0.24	0.39	0.34	0.45	0.32	0.43								60.8
SAPT2+3(CCD)	0.33	0.21	0.25	0.68	0.17	0.53								64.8
SAPT2+(CCD) $\delta$ MP2 <sup>c</sup>	0.32	0.22	0.25	0.29	0.21	0.26								58.0
SAPT2+(3)(CCD) $\delta$ MP2	0.66	0.55	0.59	0.84	0.45	0.64								60.8
SAPT2+3(CCD) $\delta$ MP2	0.55	0.46	0.49	0.71	0.38	0.53								64.8

<sup>a</sup>Errors with respect to Gold Standard (see Sec. II E for plot details). Guide lines are at 0, 0.3, and 1.0 kcal/mol overbound (−) and underbound (+).

<sup>b</sup>Time (hours) to compute adenine · thymine complex. See also Ref. 70.

<sup>c</sup>SAPT2+(CCD) $\delta$ MP2 and MP2(CCD) are identical in IE.

DD systems, MP2 tends to overestimate interaction energies, and hence it performs better for smaller basis sets, where there can be a favorable cancellation of errors; on the other hand, for less polarizable systems like methane dimer, larger basis sets work better for MP2.<sup>27</sup> Similarly, the cancellation of errors for SAPT0 is best in small basis sets for more polarizable systems.

The relatively poor overall performance of SAPT0 for hydrogen-bonded complexes is notable, even with its optimal jaDZ basis set. As seen in Table III, nearly all hydrogen bonded complexes are overbound at SAPT0/jaDZ, and some have errors >3 kcal mol<sup>-1</sup>. These errors can be

remedied to some extent by using *s*SAPT0. As defined in Eqs. (6) and (7), *s*SAPT0 is SAPT0 with corrections for the *S*<sup>2</sup> approximation depending on the ratio of *E*<sub>exch</sub><sup>(10)</sup> to *E*<sub>exch</sub><sup>(10)</sup>(*S*<sup>2</sup>). The *s*SAPT0/jaDZ method decreases HB MAE from 0.80 to 0.49 kcal mol<sup>-1</sup> for the S22 database and from 1.26 to 0.71 kcal mol<sup>-1</sup> across all four databases relative to SAPT0/jaDZ. This correction more dramatically reduces maximum HB error of SAPT0/jaDZ from −6.68 kcal mol<sup>-1</sup> down to −1.55 kcal mol<sup>-1</sup> for *s*SAPT0/jaDZ. MX/DD remain virtually unchanged with a good MAE for both SAPT0 and *s*SAPT0 (0.32 and 0.31 kcal mol<sup>-1</sup>). As with SAPT0, the minimum errors for *s*SAPT0 occur with the jaDZ basis set.

TABLE V. Mean absolute error (kcal mol<sup>-1</sup>) of the interaction energy for databases and their subsets with aug-cc-pVQZ and aug-cc-pV5Z basis sets. Full tables for all SAPT methods and basis sets located in the supplementary material.<sup>63</sup>

Method & Basis Set	S22			Overall			Error Distribution <sup>a</sup>							Time <sup>b</sup>
	HB	MX/DD	TT	HB	MX/DD	TT	4	OB	1	0	1	UB	4	
aug-cc-pVQZ														
DFT-SAPT	0.76	0.18	0.36	0.69	0.15	0.31								93.7 <sup>b</sup>
SAPT0	2.96	1.63	2.05	3.66	1.20	2.49								4.5
sSAPT0	2.61	1.60	1.92	2.98	1.17	2.08								4.5
aug-cc-pV5Z														
SAPT0	3.01	1.66	2.09	3.73	1.22	2.54								30.0
sSAPT0	2.67	1.63	1.96	3.05	1.20	2.12								30.0

<sup>a</sup>Errors with respect to Gold Standard (see Sec. II E for plot details). Guide lines are at 0, 0.3, and 1.0 kcal/mol overbound (−) and underbound (+).<sup>b</sup>Time (hours) to compute adenine · thymine complex. See also Ref. 70.

Spin-component scaling does not notably improve the performance of SAPT0. Using jaDZ, SAPT0 and SCS-SAPT0 have nearly identical total errors, with SCS-SAPT0 improving HB slightly and worsening MX/DD by a similar amount ( $\sim 0.1$  kcal mol<sup>-1</sup> MAE), thus cancelling overall. In larger double- $\zeta$  basis sets, SCS-SAPT0 does outperform SAPT0 slightly by  $\sim 0.3$  kcal mol<sup>-1</sup> overall MAE; however, no SCS-SAPT0 model chemistry outperforms SAPT0/jaDZ, much less sSAPT0/jaDZ.

## B. DFT-SAPT

DFT-SAPT/aTZ has excellent performance for MX/DD complexes (0.15 kcal mol<sup>-1</sup> overall MAE) and moderate performance for HB complexes (0.92 kcal mol<sup>-1</sup> MAE). Double- $\zeta$  basis sets do not demonstrate strong performance, as their errors are at least twice those of aTZ. HB MAE can be further decreased to 0.69 kcal mol<sup>-1</sup> by going to the quadruple- $\zeta$  aQZ, whereas MX/DD MAE remain the same as aTZ. These data as well as the much larger time requirement for aQZ (see Sec. III F) lead us to recommend DFT-SAPT/aTZ as the optimal DFT-SAPT model chemistry.

DFT-SAPT generally underbinds HB complexes, but increasing the basis set size monotonically improves HB error performance. At the largest basis set examined, aQZ, HB complexes are still considerably underbound and are unlikely to reach the very low MX/DD errors which large-basis DFT-SAPT displays. We did not pursue an analogous exchange-scaling method to improve the HB performance of DFT-SAPT as was done for sSAPT0. Using a similar method would make HB errors for DFT-SAPT worse, thus we offer no recommendation for lowering the HB errors of DFT-SAPT beyond maximizing the basis set size.

## C. SAPT2, 2+, 2+(3), and 2+3

SAPT2 has an overall MAE as low as 0.74 kcal mol<sup>-1</sup> with the jaTZ basis, rivaling the accuracy of SAPT0/jaDZ, but at many times the computational cost (see Sec. III F). The overall MAE in SAPT2 is little changed across all triple- $\zeta$  basis sets, as HB and MX/DD MAE fluctuate between 0.5 and 0.9 kcal mol<sup>-1</sup>. SAPT2/aTZ has a MAE which is  $>2$  times

larger than DFT-SAPT/aTZ (0.82 vs. 0.38 kcal mol<sup>-1</sup>), which is of the same order-of-magnitude of computational effort. We shall also see that SAPT2 does not perform nearly as well in triple- $\zeta$  basis sets as other high-order wavefunction-based SAPT methods. Thus, we do not recommend the SAPT2 method for general applications.

SAPT2+ completes the description of dispersion to second order in both the intermolecular interaction,  $\hat{V}$ , and the intramonomer correlation,  $\hat{W}$  [involving a (T)-type term with its associated  $\mathcal{O}(N^7)$  scaling, see Sec. II A]. SAPT2+/aDZ has the lowest errors in the HB and MX/DD subsets out of all basis sets considered, with an overall MAE of 0.30 kcal mol<sup>-1</sup>. The SAPT2+/aDZ HB MAE of 0.46 kcal mol<sup>-1</sup> is the lowest HB MAE of all SAPT methods until we consider the  $\delta$ MP2 correction (discussed below). Given that this method has a Pauling point in a double- $\zeta$  basis set, SAPT2+/aDZ may be advisable for those who wish to go beyond the accuracy of sSAPT0/jaDZ but cannot afford a triple- $\zeta$  SAPT2+(3) computation.

SAPT2+(3)/aTZ is one of the top-performing wavefunction SAPT methods for MX/DD complexes, with a MAE of 0.18 kcal mol<sup>-1</sup>, competitive with the 0.14 kcal mol<sup>-1</sup> MX/DD MAE of DFT-SAPT/aTZ. Its rather high MAE of 0.79 kcal mol<sup>-1</sup> for the HB subset can be decreased to 0.24 kcal mol<sup>-1</sup> by including a  $\delta$ MP2 correction (see Sec. II A). The resulting SAPT2+(3) $\delta$ MP2/aTZ has overall MAE of 0.15 kcal mol<sup>-1</sup> (0.13 kcal mol<sup>-1</sup> MX/DD), which is among the very best for all SAPT methods studied here.

SAPT2+3 does not outperform SAPT2+(3) in large basis sets, but it is comparable to SAPT2+ in double- $\zeta$  basis sets, with SAPT2+3/aDZ showing an overall MAE of 0.28 kcal mol<sup>-1</sup>, nearly identical total error to SAPT2+/aDZ. In the aTZ basis, SAPT2+3 performs noticeably worse than SAPT2+(3) for both HB (1.24 vs. 0.79 kcal mol<sup>-1</sup>) and MX/DD (0.35 vs. 0.18, nearly a factor of two). When the  $\delta$ MP2 correction is included to remedy the large hydrogen-bonding errors, SAPT2+3 $\delta$ MP2 is nearly identical to SAPT2+(3) $\delta$ MP2, which gives excellent results for all types of complexes (0.15 kcal mol<sup>-1</sup> overall MAE).

Wavefunction SAPT methods can be very time-intensive computations, and a small decrease in the number of basis functions may be the difference between a tractable or an

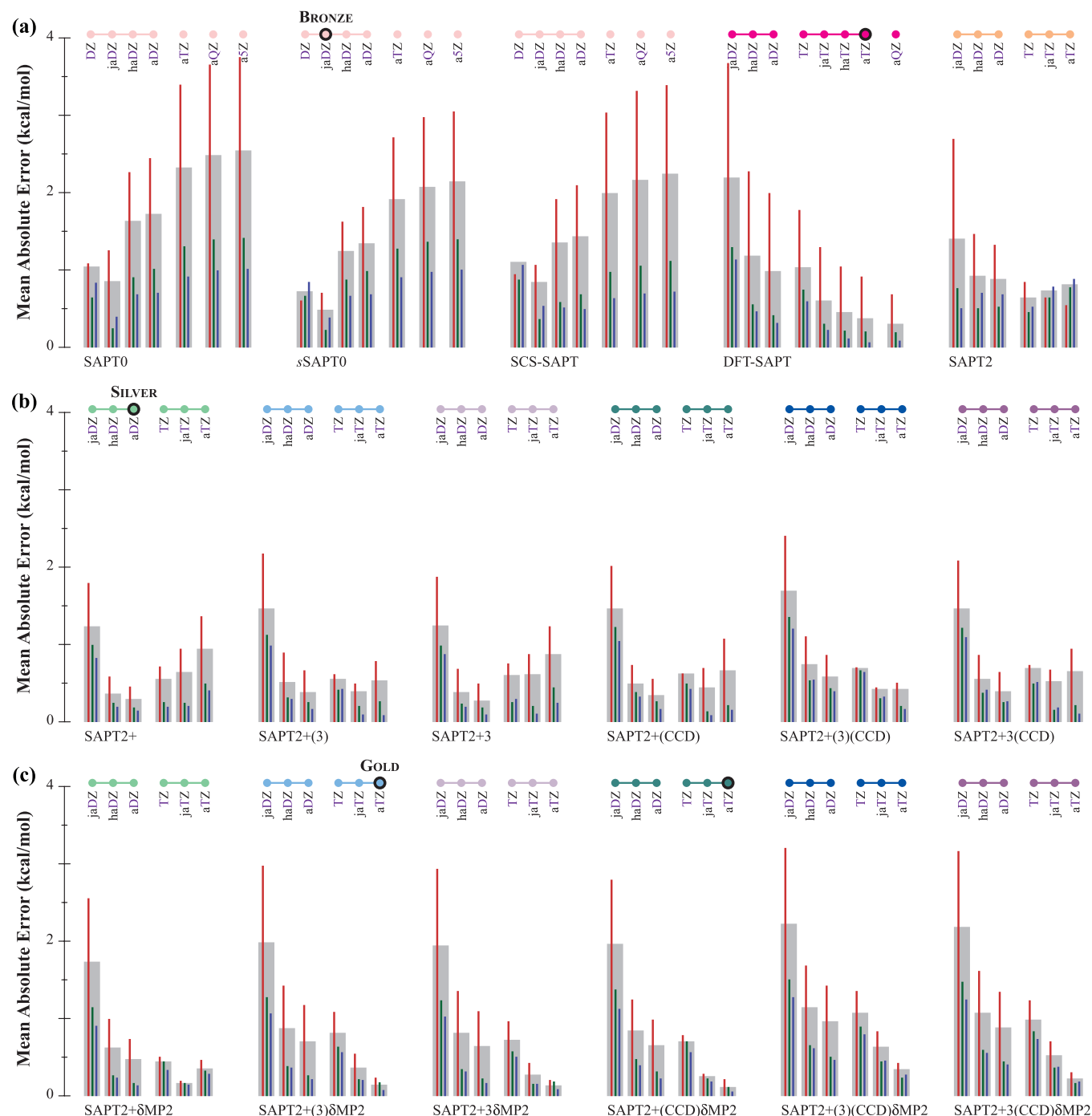


FIG. 2. Performance of SAPT methods. For each technique considered among (a) zeroth- and second-order truncations, (b) higher, triples-including truncations, and (c) higher truncations with  $\delta$ MP2 corrections, the MAE averaged over four databases is plotted (gray) for smaller to larger basis sets. Subset MAE values are shown as inset bars for hydrogen-bonding (red), mixed-influence (green), and dispersion-dominated (blue) NCI motifs. Colored circles correspond to computational cost traces in Fig. 3, and black-bordered colored circles indicate Pauling points<sup>44</sup> in SAPT theory.

intractable application. For such cases, basis set truncation using the scheme of Papajak and Truhlar<sup>41</sup> may be appropriate. SAPT2+/aDZ and SAPT2+/haDZ vary slightly in their overall MAE (0.30 vs. 0.37 kcal mol<sup>-1</sup>), yet haDZ offers a 25% time savings over aDZ for adenine·thymine. Similarly, SAPT2+(3) $\delta$ MP2 retains excellent performance when truncating from aTZ to haTZ (0.15 vs. 0.21 kcal mol<sup>-1</sup>). Larger truncations to jaTZ or maTZ result in more severe deterioration of MAE, and are not recommended ex-

cept when absolutely necessary to make the computation tractable.

#### D. SAPT(CCD)

The more robust treatment of dispersion based on CCD rather than perturbation theory should in principle provide better results for molecular complexes in which dispersion dominates the interaction energy. The difficult doubly

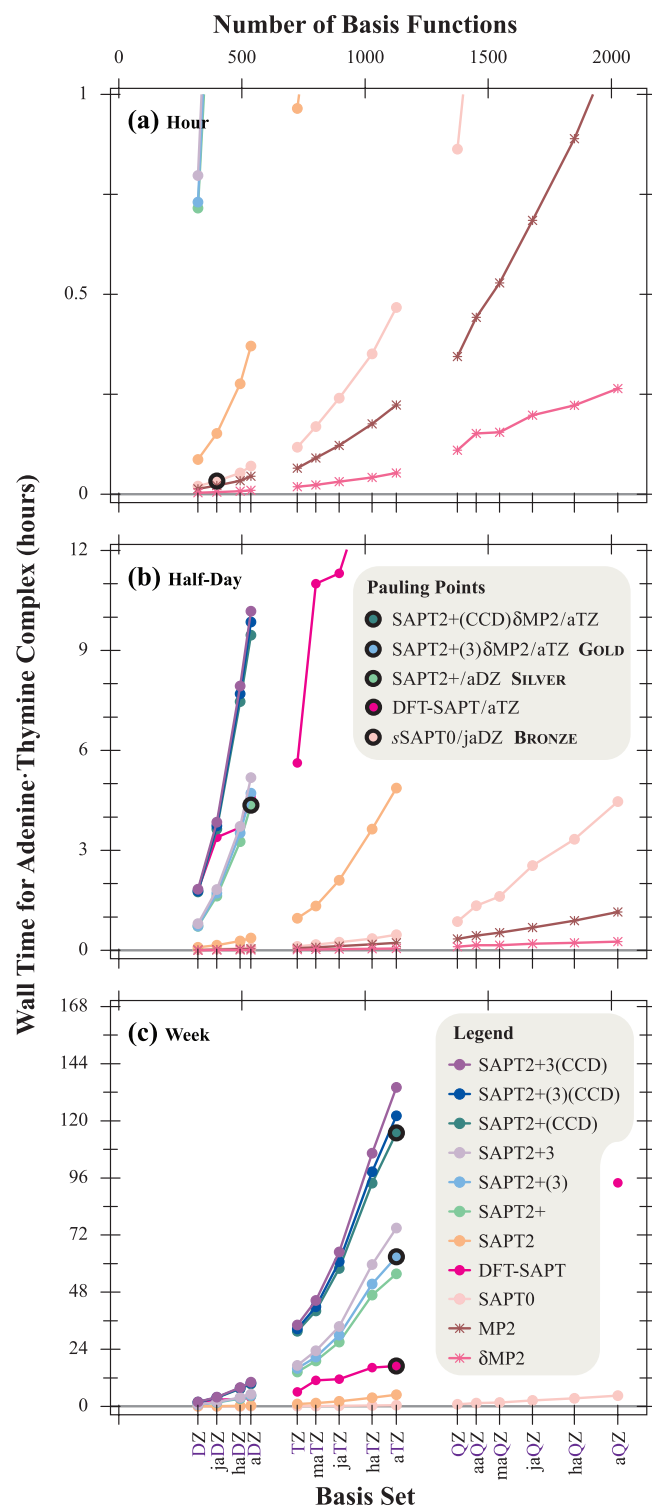


FIG. 3. Efficiency results for SAPT methods. The total wall time in hours for hydrogen-bonded adenine-thymine (S22-7) is depicted for SAPT variants between SAPT0 and SAPT2+3(CCD) in complexity and for basis sets between cc-pVDZ and aug-cc-pVQZ in size. Panels show the model chemistries accessible in (a) an hour, (b) half a day, and (c) a week. See also Ref. 70 on comparability of DFT-SAPT.

hydrogen-bonded complexes of the HBC6 database also stand to benefit from a better description of dispersion, as large errors occur when monomers approach very close to one another, which can produce a large dispersion energy.

Among SAPT2+, SAPT2+(3), and SAPT2+3 methods, we see in Fig. 2(b) the disturbing trend that HB errors increase with basis set size going from aDZ to aTZ (MX and DD as well for SAPT2+ and SAPT2+3). Electronic structure methods should have diminishing errors with increasing basis set size if their treatment of electron correlation is accurate. Using CCD dispersion eliminates or significantly reduces this effect in these wavefunction SAPT methods, although the trend remains to a certain degree for HB complexes in SAPT2+.

SAPT2+(CCD) is an improvement over SAPT2+ in triple- $\zeta$  basis sets; however, SAPT2+(CCD) does not outperform SAPT2+/aDZ in terms of MAE using any of the basis sets considered here. SAPT2+(CCD) becomes more accurate with larger basis sets for MX/DD complexes, with a MX/DD MAE of 0.19 kcal mol<sup>-1</sup> for SAPT2+(CCD)/aTZ. However, the large HB MAE of 1.08 kcal mol<sup>-1</sup> rules out SAPT2+(CCD)/aTZ as a Pauling point, given the much better 0.46 kcal mol<sup>-1</sup> HB MAE of the non-CCD variant SAPT2+/aDZ.

SAPT2+(3)(CCD)/aTZ retains the accuracy of SAPT2+(3)/aTZ for MX/DD (0.19 kcal mol<sup>-1</sup> MAE), while improving HB MAE from 0.79 to 0.51 kcal mol<sup>-1</sup> for an overall MAE of 0.43 kcal mol<sup>-1</sup>. SAPT2+(3)(CCD) also has the attractive feature that the error for each binding motif subset decreases nearly monotonically with increasing basis set size. While its overall performance is similar to SAPT2+/aDZ, SAPT2+(3)(CCD)/aTZ outperforms SAPT2+/aDZ for all S22 subsets, suggesting superior performance for equilibrium complexes.

SAPT2+3(CCD)/aTZ performs similarly to SAPT2+(3)/aTZ for MX/DD complexes, but it falls short for HB complexes (0.95 vs. 0.79 kcal mol<sup>-1</sup> HB MAE). SAPT2+3(CCD) mirrors SAPT2+(CCD) very closely in all basis sets, with smoothly decreasing and excellent MX/DD errors in large basis sets, but with HB errors which become quite large in triple- $\zeta$  basis sets.

## E. SAPT $\delta$ MP2

The most accurate and robust methods studied here are those which utilize the  $\delta$ MP2 correction. This is due in part to the failure of SAPT-based perturbation theory methods at short-range intermolecular contacts, which results in large errors for the short-range part of the Hydrogen-Bonded Curves (HBC6) database. We observe larger HB than MX/DD errors for nearly every SAPT model chemistry, despite the fact that MX/DD interaction energies can be quite difficult for electronic structure methods to model reliably due to the need for high-accuracy electron-correlation treatment. The  $\delta$ MP2 correction was designed here to remedy this deficiency, which it does quite well, at the expense of the unambiguous decomposition of the interaction energy into physical terms, as  $\delta$ MP2 includes both induction and dispersion character. We have chosen to include this quantity, which is typically small for the cases considered here, in the induction component. However, for complexes in which this correction is significant, the breakdown of perturbation theory may be large enough that it

is no longer possible to compute the separate physical energy contributions with high accuracy.

The  $\delta$ MP2-including methods (except for SAPT2+ $\delta$ MP2) all display monotonic convergence towards the complete basis set limit [see Fig. 2(c)] and yield the smallest MAE with the largest basis sets for both HB and MX/DD complexes. This is to be expected, as these methods are all supermolecular MP2 plus a handful of additional SAPT terms (nearly all dispersion), and Dunning basis sets were designed to allow correlated methods such as supermolecular MP2 to smoothly converge towards the complete basis set limit. Additionally, the difference between HB and MX/DD errors diminishes as basis set size increases, with HB and MX/DD errors being nearly equal for most  $\delta$ MP2 methods by the aTZ basis set.

SAPT2+(3) $\delta$ MP2/aTZ and SAPT2+3 $\delta$ MP2/aTZ are nearly equivalent model chemistries with excellent errors for HB (0.24 and 0.21 kcal mol<sup>-1</sup>) and MX/DD (0.13 and 0.14 kcal mol<sup>-1</sup>) complexes. SAPT2+ $\delta$ MP2/aTZ does not perform quite as well, with an overall MAE of 0.36 kcal mol<sup>-1</sup>.

CCD dispersion amplitudes may be used in conjunction with  $\delta$ MP2 methods, with mixed results. For SAPT2+(3) and SAPT2+3, adding the CCD correction to  $\delta$ MP2 methods produces methods which perform slightly worse than the non-CCD variants. SAPT2+(3)(CCD) $\delta$ MP2/aTZ and SAPT2+3(CCD) $\delta$ MP2/aTZ each perform 0.1–0.2 kcal mol<sup>-1</sup> worse overall MAE than SAPT2+(3) $\delta$ MP2/aTZ and SAPT2+3 $\delta$ MP2/aTZ, respectively.

Conversely, SAPT2+(CCD) $\delta$ MP2 provides the most accurate overall model chemistry considered in the present study. Because this method is essentially a supermolecular MP2 computation supplemented with a dispersion correction from CCD amplitudes, we refer to this method in shorthand as MP2(CCD). MP2(CCD) performs best in the aTZ basis set, with an overall HB error of 0.22 kcal mol<sup>-1</sup> and an overall error of 0.12 kcal mol<sup>-1</sup>. This model chemistry outperforms the next best performers of SAPT2+3 $\delta$ MP2/aTZ, SAPT2+(3)(CCD)/aTZ, and DFT-SAPT/aTZ in all six statistical categories presented in Table IV.

## F. Examination of computational efficiency

Figure 3 displays the time required to compute the interaction energy of hydrogen-bonded adenine·thymine with various SAPT model chemistries (see Sec. III F for more details). DFT-SAPT is an anomaly on this figure, as DFT-SAPT in MOLPRO uses serial computation, rather than the parallel computation in PSI4 used for wavefunction-based SAPT. We see from the three subsections of Fig. 3 that computation time spans several orders of magnitude, from minutes to weeks. The MP2 point indicates time for an entire supermolecular MP2 computation including Hartree–Fock computations. The  $\delta$ MP2 point indicates the time for only the MP2 correlation portion, as a supermolecular Hartree–Fock computation is already necessary for every SAPT computation.

SAPT0 is the most efficient SAPT method considered here by far, with a 2026 basis function adenine·thymine SAPT0/aQZ computation taking only a few hours to

complete. This computation takes comparable effort to SAPT2+3/aDZ which has 4 times fewer basis functions (536), or SAPT2+3(CCD)/jaDZ with only 397 basis functions. This high efficiency allowed for computation of all benchmark database members up to SAPT0/a5Z without difficulty. The relevant SAPT0 Pauling point at jaDZ takes only  $\sim 2$  min to complete, making this a very attractive method for quick qualitative insight into the physical nature of non-covalently bound complexes of up to a few hundred atoms.

SAPT2 takes a factor of  $\sim 5$  longer to complete than SAPT0 at aDZ and a factor of  $\sim 10$  at aTZ. The greater computational effort required and the failure of any SAPT2-based level of theory to beat the accuracy of SAPT0/jaDZ on average leads us to recommend against the application of SAPT2.

SAPT2+, SAPT2+(3), and SAPT2+3 differ by only a few terms and thus are tightly bunched in Fig. 3. Relative to SAPT0/jaDZ, each method requires 2 orders of magnitude more time with the aDZ basis set, and 3 orders of magnitude more time with the aTZ basis set. These methods require larger basis sets than SAPT0 to reach their lowest observed overall MAE, such as SAPT2+/aDZ or SAPT2+(3)/aTZ. Completing the adenine·thymine computation for one of these methods with aTZ (1127 basis functions) requires multiple days. This is approaching the tractability limit of SAPT2+ and beyond, given the steep  $O(N^7)$  scaling of these methods.

SAPT(CCD) computations require approximately twice as much computing time as their non-CCD counterparts. The additional time required for SAPT2+, SAPT2+(3), and SAPT2+3 to achieve the corresponding (CCD) method lies in 5 CCD-type computations. Natural orbital truncations within these CCD computations allow for the simple factor of 2 increase in computation time, which makes the tractability limit for SAPT2+3(CCD) nearly the same as that of SAPT2+3. The SAPT2+3(CCD)/aTZ adenine·thymine computation is the most demanding performed in this study, requiring  $\sim 5.5$  days to complete. SAPT2+(CCD)/aTZ and SAPT2+(3)(CCD)/aTZ also take  $\sim 5$  days.

One can clearly see from Fig. 3 that the  $\delta$ MP2 correction is functionally free relative to the cost of the SAPT2+, SAPT2+(3), or SAPT2+3 computation on top of which it is applied ( $<1\%$  of total computation time). Thus, when we see similar errors between a SAPT(CCD) and a SAPT $\delta$ MP2 method, the latter is advisable as a more time-efficient choice when interaction energy accuracy is the sole criterion.

## G. Comparison to supermolecular approaches

Figure 4 provides a comparison of the best SAPT model chemistries discussed above to a few common supermolecular model chemistries. In-depth analysis of density functional<sup>30</sup> and wavefunction<sup>31,69</sup> supermolecular model chemistries may be found elsewhere, and we make only a quick comparison here for the benefit of the reader. We again stress that supermolecular methods do not provide the decomposition of the interaction energy into physical components as do SAPT methods. Wavefunction model chemistries included are second-order Møller–Plesset perturbation theory (MP2) and its standard spin-component scaled<sup>12</sup> variant (SCS-MP2),



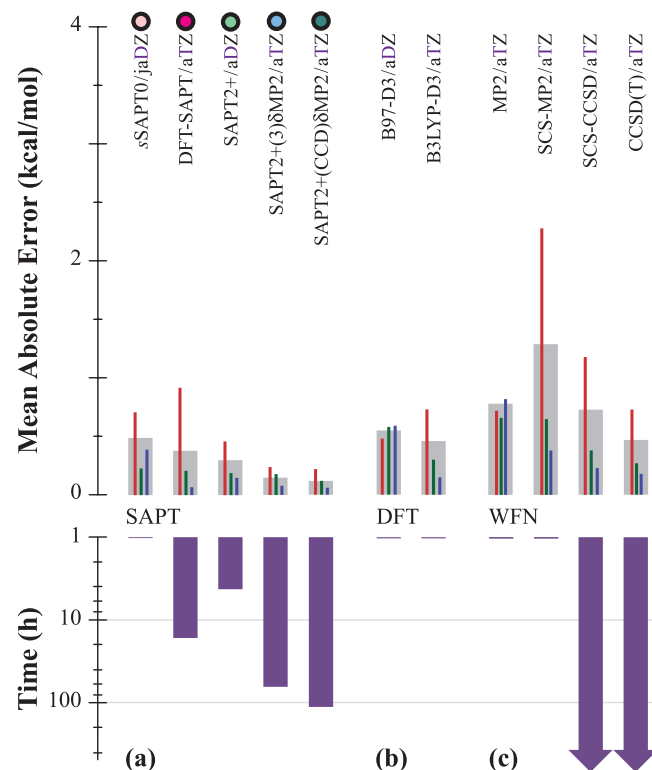


FIG. 4. Comparison of SAPT to supermolecular methods. The (a) recommended SAPT model chemistries are compared to common (b) density functional and (c) wavefunction approaches according to both efficiency (purple; time required for adenine · thymine) and accuracy (gray; MAE averaged over four databases) metrics. Subset MAE values are shown as inset bars for hydrogen-bonding (red), mixed-influence (green), and dispersion-dominated (blue) NCI motifs.

as well as SCS-CCSD<sup>48</sup> and CCSD(T), all in the aTZ basis. We also include two of the best performing DFT model chemistries for non-covalent interactions,<sup>30</sup> B97-D3/aDZ<sup>10,11</sup> and B3LYP-D3/aTZ. Wavefunction model chemistries are counterpoise-corrected, whereas DFT model chemistries are not.

All five most recommended SAPT model chemistries have a lower overall MAE than both MP2/aTZ and SCS-MP2/aTZ. Even the very efficient *s*SAPT0/jaDZ has a slightly lower MAE with only 1/4 of the computational cost (see Sec. II D and Table III). This difference comes from not only the larger basis set but from the necessity to compute both dimer and monomer systems for supermolecular methods. All SAPT model chemistries in Fig. 4 also outperform SCS-CCSD/aTZ, while requiring only a fraction of the CPU time. Both DFT approaches B97-D3/aDZ and B3LYP-D3/aTZ have similar overall MAE to *s*SAPT0/jaDZ, although at a factor of 4 and 10 larger computational cost for adenine · thymine, respectively, primarily due to the larger basis sets. More advanced SAPT Pauling Points have a lower MAE than these DFT model chemistries, although at a much greater cost.

## H. Recommendations for applications

Given the accuracy and timings data presented above, we can make recommendations for a hierarchy of SAPT methods for chemical applications. The following is a list of SAPT model chemistries which provide increasingly accurate interaction energies (overall MAE in kcal mol<sup>-1</sup>):

$$\begin{aligned} \text{SAPT0/jaDZ (0.86)} &< \text{SAPT2+(3)/aTZ (0.54)} \sim \text{sSAPT0/jaDZ (0.49)} \\ &\sim \text{SAPT2+(3)(CCD)/aTZ (0.43)} < \text{DFT-SAPT/aTZ (0.38)} \sim \text{SAPT2+/aDZ (0.30)} \\ &< \text{SAPT2+(3)\delta MP2/aTZ (0.15)} \sim \text{MP2(CCD)/aTZ (0.12)} \end{aligned}$$

When ranking these same eight best model chemistries by overall HB MAE we obtain the following rankings (kcal mol<sup>-1</sup>):

$$\begin{aligned} \text{SAPT0/jaDZ (1.26)} &< \text{DFT-SAPT/aTZ (0.92)} < \text{SAPT2+(3)/aTZ (0.79)} \\ &\sim \text{sSAPT0/jaDZ (0.71)} < \text{SAPT2+(3)(CCD)/aTZ (0.51)} \sim \text{SAPT2+/aDZ (0.46)} \\ &< \text{SAPT2+(3)\delta MP2 (0.24)} \sim \text{MP2(CCD)/aTZ (0.22)} \end{aligned}$$

When ranking these eight model chemistries by MX/DD MAE we obtain these rankings (kcal mol<sup>-1</sup>):

$$\begin{aligned} \text{SAPT0/jaDZ (0.32)} &\sim \text{sSAPT0/jaDZ (0.31)} < \text{SAPT2+(3)(CCD)/aTZ (0.19)} \\ &\sim \text{SAPT2+(3)/aTZ (0.18)} \sim \text{SAPT2+/aDZ (0.17)} \sim \text{DFT-SAPT/aTZ (0.14)} \\ &\sim \text{SAPT2+(3)\delta MP2 (0.13)} \sim \text{MP2(CCD)/aTZ (0.09)} \end{aligned}$$

We can then rank these methods by computational efficiency (hours for adenine · thymine computation):

$$\begin{aligned} \text{SAPT2+(3)(CCD)/aTZ (122.1)} &< \text{MP2(CCD)/aTZ (114.9)} < \text{SAPT2+(3)\delta MP2/aTZ} \\ &(62.9) \sim \text{SAPT2+(3)/aTZ (62.9)} < \text{DFT-SAPT/aTZ (16.8)}^{70} < \text{SAPT2+/aDZ (4.4)} \\ &\ll \text{sSAPT0/jaDZ (0.03)} = \text{SAPT0/jaDZ (0.03)} \end{aligned}$$

Comparing these lists, we see that *s*SAPT0/jaDZ provides the best error per unit computational effort by far, taking only a few minutes, yet providing an overall MAE which is competitive with the very robust SAPT2+(3)(CCD)/aTZ. SAPT2+/aDZ is competitive with the very accurate DFT-SAPT with either the aTZ or aQZ basis set for MX/DD complexes, while outperforming both for HB complexes, and at a lower computational cost.<sup>70</sup> SAPT2+(3) $\delta$ MP2/aTZ is also very near the top of the list, yet costs only half the time of the best model chemistry, MP2(CCD)/aTZ, due to the time required for the needed CCD computations. Given this data, we recommend the following methods as gold, silver, and bronze standards for Symmetry-Adapted Perturbation Theory applications:

**Gold:** SAPT2+(3) $\delta$ MP2/aTZ (0.15 kcal mol<sup>-1</sup> overall MAE, 62.9 h for A · T),

**Silver:** SAPT2+/aDZ (0.30 kcal mol<sup>-1</sup> overall MAE, 4.4 h for A · T),

**Bronze:** *s*SAPT0/jaDZ (0.49 kcal mol<sup>-1</sup> overall MAE, 0.03 h for A · T).

If one seeks a quick qualitative answer, *s*SAPT0/jaDZ does the job well. This accuracy can be improved upon by nearly a factor of two with two orders of magnitude more effort by using SAPT2+/aDZ. The highest tier of accuracy can be obtained with an additional order of magnitude of effort which will more than halve the error again with SAPT2+(3) $\delta$ MP2/aTZ, achieving an interaction energy whose quantitative accuracy approaches that of the best quantum chemistry methods which are tractable for the given system.

#### IV. SUMMARY AND CONCLUSIONS

Computational prediction of the strength and orientation of various non-covalent interactions is critical for the next generation of development in pharmaceutical drug design, protein folding, nanotechnology, and electronic materials design. SAPT provides a straightforward way to both obtain an interaction energy and examine its physical components. Here we have provided a systematic examination of the computational efficiency and accuracy for computing interaction energies of SAPT methods in combination with many basis sets. Accuracy was assessed relative to high-quality CCSD(T)/CBS reference values, across four databases of various binding motifs, including examples from doubly hydrogen-bonded formic acid dimer, to mixed-influence benzene · water, to dispersion-dominated benzene dimer.

SAPT methods surveyed include SAPT0, SAPT2, DFT-SAPT, SAPT2+, SAPT2+(3), and SAPT2+3. We use the latter three methods with and without dispersion from coupled-cluster doubles  $t_2$  amplitudes, as well as with and without a  $\delta$ MP2 correction from the supermolecular MP2 interaction energy. Note that we use and recommend for general applications an “exchange-scaling” based on the ratio between  $E_{\text{exch}}^{(10)}$  with and without the  $S^2$  approximation ( $\alpha = 1.0$ ).<sup>50</sup> The

newly defined “*s*SAPT0” method uses exchange-scaling with  $\alpha = 3.0$ .

We examine Dunning’s correlation-consistent basis sets ranging in size from cc-pVDZ to aug-cc-pV5Z wherever computationally tractable for the largest bimolecular complex in our databases (adenine · thymine). We also examine the effect of truncating diffuse functions according to the calendar-month scheme of Papajak and Truhlar<sup>41</sup> (defined in Table I). All model chemistries studied here will be available in the next public release of PSI4.

A summary of most interesting findings for various model chemistries (method + basis set) is presented below [values in parentheses are MAE in kcal mol<sup>-1</sup> across four benchmark databases (S22, HBC6, NBC10, and HSG) either overall (by default) or for the listed HB or MX/DD binding motif subset]:

1. SAPT0/jaDZ (0.86) performs qualitatively well for MX/DD complexes (0.32) but struggles with HB complexes (1.26).
2. *s*SAPT0/jaDZ (0.49) greatly improves HB errors (0.71) versus SAPT0 without affecting MX/DD errors (0.31), making it our “bronze standard” SAPT Pauling point.
3. SCS-SAPT0 does not significantly outperform SAPT0/jaDZ with any basis set or choice of SCS parameters.
4. DFT-SAPT/aTZ (0.38) has excellent performance for MX/DD complexes (0.14) but not for HB (0.92), although larger basis sets (aQZ) can somewhat improve HB performance (0.69).
5. SAPT2 does not outperform *s*SAPT0/jaDZ (which requires less CPU time) in any basis set. No SAPT2 model chemistry is recommended.
6. SAPT2+/aDZ (0.30) outperforms *s*SAPT0/jaDZ by nearly a factor of 2 at a cost of two orders of magnitude in CPU time. It is our “silver standard” SAPT Pauling point.
7. SAPT2+(3)/aTZ (0.54) performs very well for MX/DD complexes (0.18) but not so for HB cases (0.79).
8. SAPT2+(3) $\delta$ MP2/aTZ (0.15) resolves the difficulty of SAPT2+(3)/aTZ for HB (0.24), while slightly improving MX/DD (0.13), thus performing great overall, making it our “gold standard” SAPT Pauling point.
9. SAPT2+3/aDZ performs nearly identically to SAPT2+/aDZ (0.28 vs. 0.30) although at a 20% increased CPU cost. SAPT2+3/aTZ performs worse than SAPT2+(3)/aTZ (0.88 vs. 0.54), thus we recommend no general SAPT2+3 model chemistry.
10. SAPT2+(CCD) $\delta$ MP2/aTZ [also referred to as MP2(CCD)] very slightly outperforms SAPT2+(3) $\delta$ MP2/aTZ (0.12 vs. 0.15) to be the best performing SAPT method tested, but at nearly twice the computational cost, thus we award “gold standard” to the latter.

#### ACKNOWLEDGMENTS

The authors are grateful to Dr. Edward G. Hohenstein for his many contributions to SAPT methods and the PSI4

package which made this work possible. This work was supported by a research grant provided by the United States National Science Foundation (Grant No. CHE-1300497). Computational resources at the Center for Computational Molecular Science and Technology are supported through an NSF CRIF award (Grant No. CHE-0946869) and by Georgia Tech. R.M.P. is supported by a United States Department of Energy Computational Science Graduate Fellowship (Grant No. DE-FG02-97ER25308). A.G.R. was supported by a Research Experiences for Undergraduates (REU) in Chemistry Site Award to Georgia Tech from the National Science Foundation (Grant No. 1156657).

- <sup>1</sup>E. A. Meyer, R. K. Castellano, and F. Diederich, *Angew. Chem., Int. Ed. Engl.* **42**, 1210 (2003).
- <sup>2</sup>L. M. Salonen, M. Ellermann, and F. Diederich, *Angew. Chem., Int. Ed. Engl.* **50**, 4808 (2011).
- <sup>3</sup>N. J. Singh, H. M. Lee, I. Hwang, and K. S. Kim, *Supramol. Chem.* **19**, 321 (2007).
- <sup>4</sup>K. Müller-Dethlefs and P. Hobza, *Chem. Rev.* **100**, 143 (2000).
- <sup>5</sup>K. E. Riley, M. Pitoňák, P. Jurečka, and P. Hobza, *Chem. Rev.* **110**, 5023 (2010).
- <sup>6</sup>C. D. Sherrill, *Acc. Chem. Res.* **46**, 1020 (2013).
- <sup>7</sup>S. Grimme, *Chem. Eur. J.* **18**, 9955 (2012).
- <sup>8</sup>T. H. Dunning, *J. Phys. Chem. A* **104**, 9062 (2000).
- <sup>9</sup>S. Grimme, *J. Comput. Chem.* **25**, 1463 (2004).
- <sup>10</sup>S. Grimme, *J. Comput. Chem.* **27**, 1787 (2006).
- <sup>11</sup>S. Grimme, J. Antony, S. Ehrlich, and H. Krieg, *J. Chem. Phys.* **132**, 154104 (2010).
- <sup>12</sup>S. Grimme, *J. Chem. Phys.* **118**, 9095 (2003).
- <sup>13</sup>O. Marchetti and H. Werner, *J. Phys. Chem. A* **113**, 11580 (2009).
- <sup>14</sup>K. Ragavachari, G. W. Trucks, J. A. Pople, and M. Head-Gordon, *Chem. Phys. Lett.* **157**, 479 (1989).
- <sup>15</sup>G. D. Purvis and R. J. Bartlett, *J. Chem. Phys.* **76**, 1910 (1982).
- <sup>16</sup>E. G. Hohenstein and C. D. Sherrill, *WIREs Comput. Mol. Sci.* **2**, 304 (2012).
- <sup>17</sup>T. J. Lee and G. E. Scuseria, *Quantum Mechanical Electronic Structure Calculations with Chemical Accuracy* (Springer, Dordrecht, 1995).
- <sup>18</sup>P. Jurečka, J. Šponer, J. Černý, and P. Hobza, *Phys. Chem. Chem. Phys.* **8**, 1985 (2006).
- <sup>19</sup>T. Takatani, E. G. Hohenstein, M. Malagoli, M. S. Marshall, and C. D. Sherrill, *J. Chem. Phys.* **132**, 144104 (2010).
- <sup>20</sup>M. S. Marshall, L. A. Burns, and C. D. Sherrill, *J. Chem. Phys.* **135**, 194102 (2011).
- <sup>21</sup>L. Gráfová, M. Pitoňák, J. Řezáč, and P. Hobza, *J. Chem. Theory Comput.* **6**, 2365 (2010).
- <sup>22</sup>J. Řezáč, K. E. Riley, and P. Hobza, *J. Chem. Theory Comput.* **7**, 2427 (2011).
- <sup>23</sup>J. Řezáč, K. E. Riley, and P. Hobza, *J. Chem. Theory Comput.* **7**, 3466 (2011).
- <sup>24</sup>K. S. Thanthirawatte, E. G. Hohenstein, L. A. Burns, and C. D. Sherrill, *J. Chem. Theory Comput.* **7**, 88 (2011).
- <sup>25</sup>M. O. Sinnokrot and C. D. Sherrill, *J. Phys. Chem. A* **110**, 10656 (2006).
- <sup>26</sup>A. L. Ringer, M. S. Figs, M. O. Sinnokrot, and C. D. Sherrill, *J. Phys. Chem. A* **110**, 10822 (2006).
- <sup>27</sup>C. D. Sherrill, T. Takatani, and E. G. Hohenstein, *J. Phys. Chem. A* **113**, 10146 (2009).
- <sup>28</sup>Y. Geng, T. Takatani, E. G. Hohenstein, and C. D. Sherrill, *J. Phys. Chem. A* **114**, 3576 (2010).
- <sup>29</sup>J. C. Faver, M. L. Benson, X. He, B. P. Roberts, B. Wang, M. S. Marshall, M. R. Kennedy, C. D. Sherrill, and K. M. Merz, *J. Chem. Theory Comput.* **7**, 790 (2011).
- <sup>30</sup>L. A. Burns, Á. Vázquez-Mayagoitia, B. G. Sumpter, and C. D. Sherrill, *J. Chem. Phys.* **134**, 084107 (2011).
- <sup>31</sup>K. E. Riley, J. A. Platts, J. Rezac, P. Hobza, and J. G. Hill, *J. Phys. Chem. A* **116**, 4159 (2012).
- <sup>32</sup>A. J. Stone, *The Theory of Intermolecular Forces*, 2nd ed. (Oxford University Press, Oxford, 2013).
- <sup>33</sup>B. Jeziorski, R. Moszynski, and K. Szalewicz, *Chem. Rev.* **94**, 1887 (1994).
- <sup>34</sup>E. G. Hohenstein and C. D. Sherrill, *J. Chem. Phys.* **132**, 184111 (2010).
- <sup>35</sup>E. G. Hohenstein and C. D. Sherrill, *J. Chem. Phys.* **133**, 014101 (2010).
- <sup>36</sup>E. G. Hohenstein, R. M. Parrish, C. D. Sherrill, J. M. Turney, and H. F. Schaefer, *J. Chem. Phys.* **135**, 174107 (2011).
- <sup>37</sup>E. G. Hohenstein and C. D. Sherrill, *J. Chem. Phys.* **133**, 104107 (2010).
- <sup>38</sup>R. M. Parrish, E. G. Hohenstein, and C. D. Sherrill, *J. Chem. Phys.* **139**, 174102 (2013).
- <sup>39</sup>H. L. Williams and C. F. Chabalowski, *J. Phys. Chem. A* **105**, 646 (2001).
- <sup>40</sup>A. J. Misquitta and K. Szalewicz, *Chem. Phys. Lett.* **357**, 301 (2002).
- <sup>41</sup>E. Papajak, J. Zheng, X. Xu, H. R. Leverentz, and D. G. Truhlar, *J. Chem. Theory Comput.* **7**, 3027 (2011).
- <sup>42</sup>M. Pitoňák, K. E. Riley, P. Neogrady, and P. Hobza, *ChemPhysChem* **9**, 1636 (2008).
- <sup>43</sup>P. Lowdin, *Int. J. Quantum Chem.* **28**, 19 (1985).
- <sup>44</sup>Strictly speaking, a Pauling point refers to a simple theoretical model which has a good agreement with experiment through cancellation of error. We use the term in this article to refer specifically to model chemistries which provide good agreement to high-quality reference data relative to computational cost.
- <sup>45</sup>B. Jeziorski, R. Moszynski, A. Ratkiewicz, S. Rybak, and K. Szalewicz, "SAPT: A program for many-body symmetry-adapted perturbation theory calculations of intermolecular interaction energies," in *Methods and Techniques in Computational Chemistry: METECC94*, Medium-Size Systems Vol. B, edited by E. Clementi (STEF, Cagliari, 1993), p. 79.
- <sup>46</sup>H. L. Williams, K. Szalewicz, R. Moszynski, and B. Jeziorski, *J. Chem. Phys.* **103**, 4586 (1995).
- <sup>47</sup>E. G. Hohenstein, "Implementation and applications of density-fitted symmetry-adapted perturbation theory," Ph.D. thesis (Georgia Institute of Technology, Atlanta, GA, 2011).
- <sup>48</sup>T. Takatani, E. G. Hohenstein, and C. D. Sherrill, *J. Chem. Phys.* **128**, 124111 (2008).
- <sup>49</sup>K. U. Lao and J. M. Herbert, *J. Phys. Chem. A* **116**, 3042 (2012).
- <sup>50</sup>Terms in turquoise-blue in Fig. 1 (i.e., all exchange-including terms except  $E_{\text{exch}}^{(10)}$ ) have applied to them an exchange-scaling factor defined both in the legend of Fig. 1 and as  $p_{\text{EX}}$  in Eq. (6). This factor depends on an exponent,  $\alpha$ , that by default is 1, the most physically justified choice. (Exchange-scaling is never applied to DFT-SAPT,  $\alpha = 0$ .) Properly, the non-unity factor of  $p_{\text{EX}}(1)$  should be present in front of each exchange term in Eqs. (2)–(5), (8), (11), (12), (17), (18), and (20) that is turquoise-blue in Fig. 1. Effectively, however, when only the total interaction energy is of interest, not the physical components, scaling by  $p_{\text{EX}}$  is largely canceled out by  $\delta E_{\text{HF}}$  or  $\delta E_{\text{MP2}}$ . [Exchange-scaling is *wholly* canceled for SAPT2+ $\delta\text{MP2}$ , SAPT2+(CCD) $\delta\text{MP2}$ , SAPT2+(3) $\delta\text{MP2}$ , and SAPT2+(3)(CCD) $\delta\text{MP2}$ .] Reading off Fig. 1, exchange-scaling is canceled whenever the term is within the blue-shaded shape bounding the HF IE or (if  $\delta\text{MP2}$  is applied) is within the pink-shaded shape bounding the MP2 correlation IE. For example, one need only scale  $E_{\text{exch-disp}}^{(20)}$  to reproduce SAPT0 results in this work or  $E_{\text{exch-disp}}^{(30)}$  to reproduce SAPT2+3 $\delta\text{MP2}$ . Wavefunction-SAPT methods where  $\alpha \neq 1$  are designated sSAPT. The only useful such method is sSAPT0 (exchange-scaled variants of higher order SAPT levels were considered and rejected) that employs  $\alpha = 3$  to scale the two exchange terms while evaluating  $\delta E_{\text{HF}}^{(2)}$  with  $\alpha = 1$  so as to not cancel out  $E_{\text{exch-ind}}^{(20)}$ .
- <sup>51</sup>E. G. Hohenstein, H. M. Jaeger, E. J. Carrell, G. S. Tschumper, and C. D. Sherrill, *J. Chem. Theory Comput.* **7**, 2842 (2011).
- <sup>52</sup>R. Bukowski, W. Cencek, P. Jankowski, B. Jeziorski, M. Jeziorska, T. Korona, S. A. Kucharski, V. F. Lotrich, A. J. Misquitta, R. Moszynski, K. Patkowski, R. Podeszwa, F. Rob, S. Rybak, K. Szalewicz, H. L. Williams, R. J. Wheatley, P. E. S. Wormer, and P. S. Zuchowski, SAPT2012: An *ab initio* program for many-body symmetry-adapted perturbation theory calculations of intermolecular interaction energies. See <http://www.physics.udel.edu/~szalewic/SAPT>.
- <sup>53</sup>K. Patkowski, K. Szalewicz, and B. Jeziorski, *J. Chem. Phys.* **125**, 154107 (2006).
- <sup>54</sup>S. F. Boys and F. Bernardi, *Mol. Phys.* **19**, 553 (1970).
- <sup>55</sup>A. Hesselmann and G. Jansen, *Phys. Chem. Chem. Phys.* **5**, 5010 (2003).
- <sup>56</sup>A. Heßelmann, G. Jansen, and M. Schütz, *J. Chem. Phys.* **122**, 014103 (2005).
- <sup>57</sup>A. J. Misquitta, B. Jeziorski, and K. Szalewicz, *Phys. Rev. Lett.* **91**, 033201 (2003).
- <sup>58</sup>A. J. Misquitta, R. Podeszwa, B. Jeziorski, and K. Szalewicz, *J. Chem. Phys.* **123**, 214103 (2005).
- <sup>59</sup>R. Podeszwa, *J. Chem. Phys.* **132**, 044704 (2010).

- <sup>60</sup>T. H. Dunning, *J. Chem. Phys.* **90**, 1007 (1989).
- <sup>61</sup>R. A. Kendall, T. H. Dunning, and R. J. Harrison, *J. Chem. Phys.* **96**, 6796 (1992).
- <sup>62</sup>E. Papajak and D. G. Truhlar, *J. Chem. Theory Comput.* **7**, 10 (2011).
- <sup>63</sup>See supplementary material at <http://dx.doi.org/10.1063/1.4867135> for tables elaborating the reference CBS extrapolation level for individual database members; defining summary error statistics; replicating Tables III–V in unabridged format; summarizing SAPT model chemistries over all databases; compiling subset results for each database and model chemistry; and a staggering number of tables detailing interaction energies.
- <sup>64</sup>It has come to our attention that SAPT results for the S22 database in the supplementary material of Ref. 65 were mislabeled; the values are SAPT2+/aug-cc-pVDZ while the implied label is SAPT2+(3)/aug-cc-pVTZ. For actual S22 SAPT2+(3)/aug-cc-pVTZ interaction energies and components, consult Tables 27 and 101 in the supplementary material of this work.
- <sup>65</sup>J. C. Flick, D. Kosenkov, E. G. Hohenstein, C. D. Sherrill, and L. V. Slipchenko, *J. Chem. Theory Comput.* **8**, 2835 (2012).
- <sup>66</sup>J. M. Turney, A. C. Simmonett, R. M. Parrish, E. G. Hohenstein, F. A. Evangelista, J. T. Fermann, B. J. Mintz, L. A. Burns, J. J. Wilke, M. L. Abrams, N. J. Russ, M. L. Leininger, C. L. Janssen, E. T. Seidl, W. D. Allen, H. F. Schaefer, R. A. King, E. F. Valeev, C. D. Sherrill, and T. D. Crawford, *WIREs Comput. Mol. Sci.* **2**, 556 (2012).
- <sup>67</sup>H.-J. Werner, P. J. Knowles, G. Knizia, F. R. Manby, M. Schütz *et al.*, MOLPRO, version 2010.1, a package of *ab initio* programs, 2010, see <http://www.molpro.net>.
- <sup>68</sup>J. A. Pople, in *Energy, Structure and Reactivity: Proceedings of the 1972 Boulder Summer Research Conference on Theoretical Chemistry*, edited by D. W. Smith and W. B. McRae (Wiley, New York, 1973), p. 51.
- <sup>69</sup>L. A. Burns, M. S. Marshall, and C. D. Sherrill, “Appointing silver and bronze standards for noncovalent interactions: a comparison of spin-component-scaled (SCS), explicitly correlated (F12), and specialized wavefunction approaches” (unpublished).
- <sup>70</sup>DFT-SAPT timings are included as a qualitative gauge of efficiency. A serial mode of operation is required for that code in molpro, and although both DFT-SAPT and wavefunction SAPT jobs were run in isolation on the same workstation, wavefunction SAPT timings have the advantage of threading over six cores in psi4. The erratic efficiency traces for DFT-SAPT with respect to basis set size are largely due to the significant variation in number of cycles required to converge the monomer LHF computations.